3-kinase-dependent and-independent components. *Biochem J* **351:** 173–182

Gao PP, Sun CH, Zhou XF, DiCicco-Bloom E, Zhou R (2000) Ephrins stimulate or inhibit neurite outgrowth and survival as a function of neuronal cell type. *J Neurosci Res* **60:** 427–436

Gao PP, Yue Y, Cerretti DP, Dreyfus C, Zhou R (1999) Ephrin-dependent growth and pruning of hippocampal axons. *Proc Natl Acad Sci USA* **96:** 4073–4077

Gao PP, Yue Y, Zhang JH, Cerretti DP, Levitt P, Zhou R (1998) Regulation of thalamic neurite outgrowth by the Eph ligand ephrin-A5: implications in the development of thalamocortical projections. *Proc Natl Acad Sci USA* **95:** 5329–5334

Gao PP, Zhang JH, Yokoyama M, Racey B, Dreyfus CF, Black IB, Zhou R (1996) Regulation of topographic projection in the brain: Elf-1 in the hippocamposeptal system. *Proc Natl Acad Sci USA* **93:** 11161–11166

Habets GG, Scholtes EH, Zuydgeest D, van der Kammen RA, Stam JC, Berns A, Collard JG (1994) Identification of an invasion-inducing gene, Tiam-1, that encodes a protein with homology to GDP-GTP exchangers for Rho-like proteins. *Cell* **77:** 537–549

Henkemeyer M, Orioli D, Henderson JT, Saxton TM, Roder J, Pawson T, Klein R (1996) Nuk controls pathfinding of commissural axons in the mammalian central nervous system. *Cell* **86:** 35–46

Holash JA, Soans C, Chong LD, Shao H, Dixit VM, Pasquale EB (1997) Reciprocal expression of the Eph receptor Cek5 and its ligand(s) in the early retina. *Dev Biol* **182:** 256–269

Kawauchi T, Chihama K, Nabeshima Y, Hoshino M (2003) The *in vivo* roles of STEF/Tiam1, Rac1 and JNK in cortical neuronal migration. *EMBO J* **22:** 4190–4201

Knoll B, Zarbalis K, Wurst W, Drescher U (2001) A role for the EphA family in the topographic targeting of vomeronasal axons. *Development* **128:** 895–906

Kunda P, Paglini G, Quiroga S, Kosik K, Caceres A (2001) Evidence for the involvement of Tiam1 in axon formation. *J Neurosci* **21:** 2361–2372

Leeuwen FN, Kain HE, Kammen RA, Michiels F, Kranenburg OW, Collard JG (1997) The guanine nucleotide exchange factor Tiam1 affects neuronal morphology; opposing roles for the small GTPases Rac and Rho. *J Cell Biol* **139:** 797–807

Liebl DJ, Morris CJ, Henkemeyer M, Parada LF (2003) mRNA expression of ephrins and Eph receptor tyrosine kinases in the neonatal and adult mouse central nervous system. *J Neurosci Res* **71:** 7–22

Mann F, Ray S, Harris W, Holt C (2002) Topographic mapping in dorsoventral axis of the *Xenopus* retinotectal system depends on signaling through ephrin-B ligands. *Neuron* **35:** 461–473

Matsuo N, Hoshino M, Yoshizawa M, Nabeshima Y (2002) Characterization of STEF, a guanine nucleotide exchange factor for Rac1, required for neurite growth. *J Biol Chem* **277:** 2860–2868

Otsuki Y, Tanaka M, Yoshii S, Kawazoe N, Nakaya K, Sugimura H (2001) Tumor metastasis suppressor nm23H1 regulates Rac1 GTPase by interaction with Tiam1. *Proc Natl Acad Sci USA* **98:** 4385–4390

Palmer A, Zimmer M, Erdmann KS, Eulenburg V, Porthin A, Heumann R, Deutsch U, Klein R (2002) Ephrin B phosphorylation and reverse signaling: regulation by Src kinases and PTP-BL phosphatase. *Mol Cell* **9:** 725–737

Pandey A, Lazar DF, Saltiel AR, Dixit VM (1994) Activation of the Eck receptor protein tyrosine kinase stimulates phosphatidylinositol 3-kinase activity. *J Biol Chem* **269:** 30154–30157

Sander EE, van Delft S, ten Klooster JP, Reid T, van der Kammen RA, Michiels F, Collard JG (1998) Matrix-dependent Tiam1/Rac signaling in epithelial cells promotes either cell–cell adhesion or cell migration and is regulated by phosphatidylinositol 3-kinase. *J Cell Biol* **143:** 1385–1398

Shamah SM, Lin MZ, Goldberg JL, Estrach S, Sahin M, Hu L, Bazalakova M, Neve RL, Corfas G, Debant A, Greenberg ME (2001) EphA receptors regulate growth cone dynamics through the novel guanine nucleotide exchange factor ephexin. *Cell* **105:** 233–244

Stam JC, Sander EE, Michiels F, van Leeuwen FN, Kain HE, van der Kammen RA, Collard JG (1997) Targeting of Tiam1 to the plasma membrane requires the cooperative function of the N-terminal pleckstrin homology domain and an adjacent protein interaction domain. *J Biol Chem* **272:** 28447–28454

Stuckmann I, Weigmann A, Shevchenko A, Mann M, Huttner WB (2001) Ephrin B1 is expressed on neuroepithelial cells in correlation with neocortical neurogenesis. *J Neurosci* **21:** 2726–2737

Tanaka M, Kamo T, Ota S, Sugimura H (2003) Association of Dishevelled with Eph tyrosine kinase receptor and ephrin mediates cell repulsion. *EMBO J* **22:** 847–858

Ueki T, Nakanishi K, Asai K, Okouchi Y, Isobe I, Eksioglu YZ, Kato T, Kohno K (1993) Neurotrophic action of gliostatin on cocultured neurons with glial cells. *Brain Res* **622:** 299–302

Wahl S, Barth H, Ciossek T, Aktories K, Mueller BK (2000) Ephrin-A5 induces collapse of growth cones by activating Rho and Rho kinase. *J Cell Biol* **149:** 263–270

Walker-Daniels J, Riese DJ, Kinch MS (2002) c-Cbl-dependent EphA2 protein degradation is induced by ligand binding. *Mol cancer Res* **1:** 79–87

Wang Y, Ota S, Kataoka H, Kanamori M, Li Z, Band H, Tanaka M, Sugimura H (2002) Negative regulation of EphA2 receptor by Cbl. *Biochem Biophys Res Commun* **296:** 214–220

Yun ME, Johnson RR, Antic A, Donoghue MJ (2003) EphA family gene expression in the developing mouse neocortex: regional patterns reveal intrinsic programs and extrinsic influence. *J Comp Neurol* **456:** 203–216

Zantek ND, Azimi M, Fedor-Chaiken M, Wang B, Brackenbury R, Kinch MS (1999) E-cadherin regulates the function of the EphA2 receptor tyrosine kinase. *Cell Growth Differ* **10:** 629–638

Zimmer M, Palmer A, Kohler J, Klein R (2003) EphB–ephrin-B bi-directional endocytosis terminates adhesion allowing contact mediated repulsion. *Nat Cell Biol* **5:** 869–878

FEBS 28948

FEBS Letters 577 (2004) 339–344

Analysis of estrogen receptor α signaling complex at the plasma membrane

Kotaro Azuma[a,b], Kuniko Horie[c], Satoshi Inoue[b,c], Yasuyoshi Ouchi[b], Ryuichi Sakai[a,*]

[a]*Growth Factor Division, National Cancer Center Research Institute, 5-1-1 Tsukiji, Chuo-ku, Tokyo 104-0045, Japan*
[b]*Department of Geriatric Medicine, Graduate School of Medicine, The University of Tokyo 7-3-1, Hongo, Bunkyo-ku, Tokyo 113-8655, Japan*
[c]*Division of Gene Regulation and Signal Transduction, Research Center for Genomic Medicine, Saitama Medical School, Hidaka-shi, Saitama 350-1241, Japan*

Received 11 August 2004; revised 28 September 2004; accepted 11 October 2004

Available online 21 October 2004

Edited by Veli-Pekka Lehto

Abstract There is accumulating evidence that the estrogen receptor (ER) can transduce specific signals at the plasma membrane. We tried to clarify the biological function of ER as a signaling molecule by identifying proteins that interact with the membrane-localized ER. The activation function 1 and 2 (AF-1 and AF-2) domains of ERα with or without the membrane-targeting sequence were stably expressed in the breast cancer cell line, MCF-7. The level of tyrosine phosphorylation of AF-2 was significantly elevated by the membrane localization. By mass-spectrometry analysis, α- and β-tubulins and heat shock protein 70 were identified as the AF-1-associated proteins. Of these, tubulins are associated only with membrane-targeted AF-1.

Keywords: Estrogen receptor; Non-genomic action; Breast cancer; Tubulin; Heat shock protein 70; Tyrosine phosphorylation

1. Introduction

Estrogen plays an important role not only in physiological processes such as the development of the female organs, reproduction, bone metabolism, and vascular dilatation, but also in pathological processes such as the development of breast cancer. Human estrogen receptor α (ERα) is a member of the nuclear receptor superfamily and functions as a ligand-dependent transcription factor [1,2]. A typical nuclear receptor contains a variable N-terminal region called activation function 1 (AF-1), a conserved DNA binding domain (DBD), a hinge region, and a C-terminal ligand binding domain called activation function 2 (AF-2). Both the AF-1 and AF-2 domains of ERα are shown to have a transcriptional activation function [3], and interact with transcriptional mediators and co-factors [4–10]. More than 80% of ERα is shown to localize in the nucleus in the absence of estrogen, and more than 95% is shown to localize in the nucleus upon estrogen stimulation [11]. Thus, it has been believed that the action of estrogen is mediated by nuclear-localizing ER through the regulation of target gene transcription.

However, there are accumulating evidences that the ER can transduce specific signals through association with other molecules outside the nucleus. In vascular endothelial cells, estrogen rapidly induces nitric oxide production by activating the PI3-kinase-Akt pathway [12]. In this process, ERα is shown to interact with the p85 subunit of PI3-kinase in a ligand-dependent manner [13]. In osteoblasts, ERα is shown to mediate the anti-apoptotic effect by activating the Src/Shc/Erk (extracellular signal-related kinase) pathway, and only the AF-2 domain expressed in the cytoplasm is necessary for this function [14]. These phenomena, called non-genomic actions, are not explained by the classical genomic action of ERα because of their rapid time course and the localization of interacting molecules, and are recognized as novel functions of the ER.

Independent laboratories have reported the non-genomic action of ERα in the breast cancer-derived cell line, MCF-7 [15,16]. They all observed that estrogen rapidly induces the phosphorylation of Erk, although different modes of action of ERα are proposed. Migliaccio et al. [15] showed that the association of ERα with non-receptor tyrosine kinase c-Src is the upstream event of ERα activation and the association of two molecules is dependent on the phosphorylation of Tyr 527 in the AF-2 domain of ERα. On the other hand, Song et al. demonstrated the direct association of ERα and adaptor protein Shc. This association was shown to use the AF-1 domain of ERα and does not require the phosphorylation of Tyr 527 [16]. It seems that the paucity of endogenous ERα at the plasma membrane makes it difficult to analyze the role of ERα at the membrane. In this study, we tried to clarify the components of the signaling complex in MCF-7 cells by the targeted expression of the ERα domain fragments at the plasma membrane.

2. Materials and methods

2.1. Plasmids

A FLAG epitope-tagged ERα AF-1 domain construct was generated by amplifying the coding sequence of human ERα by PCR using primers 5′-CGTACCTCGAGATGACCATGACCCCTCCACAC-3′

* Corresponding author. Fax: +81-3-3542-8170.
E-mail address: rsakai@gan2.res.ncc.go.jp (R. Sakai).

Abbreviations: AF-1 and AF-2 domains, activation function 1 and 2 domains; BSA, bovine serum albumin; DBD, DNA binding domain; DMEM, Dulbecco's Modified Eagle's medium; EGF, epidermal growth factor; ER, estrogen receptor; Erk, extracellular signal-related kinase; FBS, fetal bovine serum; Hsp70, heat shock protein 70; LC/MS/MS, liquid chromatography tandem mass spectrometry; WCL, whole cell lysate

0014-5793/$22.00
doi:10.1016/j.febslet.2004.10.025

and 5′-CGGGATCCTATTTGTCATCGTCGTCCTTGTAGTCCT-TGGCAGATTCCATAGCC- 3′. This resulted in a fragment with an *Xho*I site (underlined), a sequence that encodes the FLAG epitope (DYKDDDDK), followed by a termination codon and a *Bam*HI site (underlined). This fragment was then digested with *Xho*I and *Bam*HI sequentially, and ligated into mammalian expression vector pcDNA3.1(−)/Myc-His B (Invitrogen).

A membrane-targeted AF-1 domain construct was generated by PCR-based site-directed mutagenesis using the AF-1 construct as a template and primers 5′-GGTAGCAACAAGAGCAAGCCCAAG-GATGCCAGCCAGCGGACCATGACCCTCCACACC- 3′ and 5′-CATCTCGAGTCTAGAGGGC. The PCR product was then digested by *Dpn*I that degrades only methylated template plasmids. As a result, the N-terminal sequence of Src kinase (MGSNKSKPKDASQ encoded by underlined 39 bp) was inserted between the *Xho*I site and the N-terminal of AF-1.

A FLAG epitope-tagged ERα AF-2 domain construct was generated using the same procedure as that of the AF-1 construct by using primers 5′-CGTACCTCGAGGCCACCATGGGCAAGAAGAACA-GCCTGGCCTT-3′ and 5′-CGGGATCCTATTTGTCATCGTCGT-CCTTGTAGTCGACTGTGGCAGGGA-3′ (*Xho*I site and *Bam*HI site are underlined). A membrane-targeted AF-2 construct was also generated by PCR-based site-directed mutagenesis using the AF-2 construct as a template and primers 5′-GGTAGCAACAA-GAGCAAGCCCAAGGATGCCAGCCAGCGGAAGAAGAACA-GCCTGGCCTT- 3′ and 5′-CATGGTGGCCTCGAGTCTAG-3′.

2.2. Cell culture and transfection

MCF-7 cells were maintained in Dulbecco's Modified Eagle's medium (DMEM) with 10% FBS at 37 °C with 5% CO_2. When estrogen stimulation was necessary, MCF-7 cells were cultured in phenol red free DMEM with 5% Charcoal/Dextran Treated FBS (HyClone) for two days. Transfection was performed using FuGENE 6 (Roche) according to the manufacturer's instructions. Clones were selected using geneticin (Sigma) at a concentration of 800 μg/ml.

2.3. Antibodies and reagents

Anti-FLAG M2 monoclonal antibody and anti-α-tubulin antibody (B-5-1-2) were purchased from Sigma. Anti-β-tubulin monoclonal antibody (D-10) was from Santa Cruz. Anti-Hsp70 monoclonal antibody was purchased from Stressgen. Anti-phosphotyrosine antibody 4G10 was purchased from Upstate Biotechnology. Anti-ERα antibody (H-184) was purchased from Santa Cruz. FITC-conjugated anti-mouse antibody was from Santa Cruz. Alexa Fluor 488 goat anti-mouse IgG and Alexa Fluor 594 goat anti-rabbit IgG were purchased from Molecular Probe. HRP-conjugated anti-mouse antibody was purchased from Amersham Pharmacia. Protein-G Sepharose was purchased from Amersham Pharmacia, β-estradiol was purchased from Sigma. Nocodazole was from Sigma.

2.4. Immunocytochemistry

Cells were grown on microscope slides in 24-well plates, washed three times with PBS, fixed with 4% paraformaldehyde/0.1 M phosphate buffer for 4 min at room temperature, washed once with PBS, and permeabilized with 0.2% Triton X-100 in PBS. After another washing with PBS and blocking with 2% (bovine serum albumin, BSA)/TBST (100 mM Tris–HCl, pH 8.0, 150 mM NaCl, and 0.05% Tween 20) for 30 min, the cells were incubated with appropriate first antibodies in 2% BSA/TBST for 1 h at room temperature. The cells were washed three times with PBS and incubated with FITC-conjugated anti-mouse antibody (1:40) in 2% BSA/TBST. After the cells were washed three times with PBS, microscope slides were mounted in 1.25% DABCO and 50% PBS and 50% glycerol and visualized using a Radiance 2100 confocal microscope (Bio-Rad). In Fig. 4B, 3% BSA, 5% goat serum in TBS were used instead of 2% BSA in TBST. Alexa Fluor 488 goat anti-mouse IgG (1:2000) and Alexa Fluor 594 goat anti-rabbit IgG (1:2000) in 3% BSA and 5% goat serum/TBS were used as the secondary antibodies in Fig. 4B.

2.5. Immunoprecipitation and immunoblotting

Cells were lysed in 1% Triton X-100 buffer (50 mM HEPES, 150 mM NaCl, 10% glycerol, 1% Triton X-100, 1.5 mM $MgCl_2$, and 1 mM EGTA, 100 mM NaF, 1 mM Na_3VO_4, 10 μg/ml aprotinin, 10 μg/ml leupeptin, 1 mM phenylmethylsulfonyl fluoride), and the protein concentration was measured using BCA Protein Assay (Pierce).

For immunoprecipitation with anti-FLAG M2 antibody, cell lysate (2 mg/ml) was mixed with anti-FLAG affinity gel (Sigma) and rotated for 2–12 h at 4 °C. After the affinity gel was washed four times with 1% Triton X-100 buffer, FLAG-tagged proteins were eluted with 0.3 M glycin HCl at pH 3.5. The elutant was removed, neutralized with 2 M Tris–HCl (pH 8.8), and then boiled in the sample buffer (0.1 M Tris–HCl, pH 6.8, 2% SDS, 0.1 M dithiothreitol, 10% glycerol, and 0.01% bromophenol blue) for 5 min and analyzed by SDS–PAGE. The gels were transferred onto a polyvinylidene difluoride membrane (Millipore) and probed by immunoblotting. Immnunoreactive proteins were visualized with a chemiluminescence reagent (Western Lighting, Perkin Elmer).

2.6. Silver staining and LC/MS/MS analysis

The SDS–PAGE gels were silver stained according to a method used previously [17].

For liquid chromatography tandem mass spectrometry (LC/MS/MS) analysis, 12 ml of cell lysate containing 36 mg of total protein was mixed with 200 μl of anti-FLAG affinity gel and rotated for 8 h at 4 °C. The affinity gel was loaded onto a chromatography column (Bio-Rad), washed with 4 ml of 1% Triton X-100 buffer, and then eluted with 0.1 M glycin HCl at pH 3.5. The elutant was separated into several fractions in chronological order and then neutralized with 2 M Tris–HCl (pH 8.8). Aliquots of these fractions were subjected to SDS–PAGE analysis, stained with SYPRO Ruby protein gel stain (Bio-Rad), and fractions with a high concentration of FLAG-tagged protein were selected for further analysis. The selected fractions were dialyzed using EasySep (TOMY) in diluted (10%) PBS and then semi-lyophilized using a SpeedVac concentrator. The concentrated samples were subjected to SDS–PAGE analysis and the gel was stained with CBB (Bio-Rad). The bands to be analyzed were dissected, digested in gel with trypsin, and subjected to LC/MS/MS analysis.

3. Results

3.1. Establishment of cell lines stably expressing a series of domain fragments of ERα in MCF-7

To analyze molecules associated with ERα at the plasma membrane, a series of domain constructs were generated and named as shown in Fig. 1A. The FLAG epitope was attached to the C-terminus of the separated AF-1 domain and the AF-2 domain of ERα. They were named AF1 and AF2, respectively. To generate membrane-targeted constructs, the membrane-localizing sequence of c-Src kinase was added to the N-terminus of AF1 and AF2. Src kinase is a non-receptor tyrosine kinase localizing at the plasma membrane with its myristoylated N-terminal sequence. The membrane-targeted ERα domain constructs were named mAF1 and mAF2, respectively. ERα has a DBD and a hinge region between the AF-1 and AF-2 domains. Nuclear localizing signals are shown to reside in the DBD and hinge region [11]; therefore, these regions were excluded from our domain constructs to ensure cytoplasmic localization.

Stable transfectants that express each domain of ERα were then established using the breast cancer cell line, MCF-7. The expression and localization of the domain fragments were confirmed by the anti-FLAG staining of cells. It was observed that AF1 and AF2 localized diffusely in the cytoplasm (Fig. 1B: b and d), whereas mAF1 and mAF2 localized at the periphery of the cells (Fig. 1B: c and e), showing the obvious effect of the membrane-targeting sequence.

3.2. Tyrosine phosphorylation of the AF-2 domain at the plasma membrane

We next investigated the relationship between the tyrosine phosphorylation of the AF-2 domain and membrane locali-

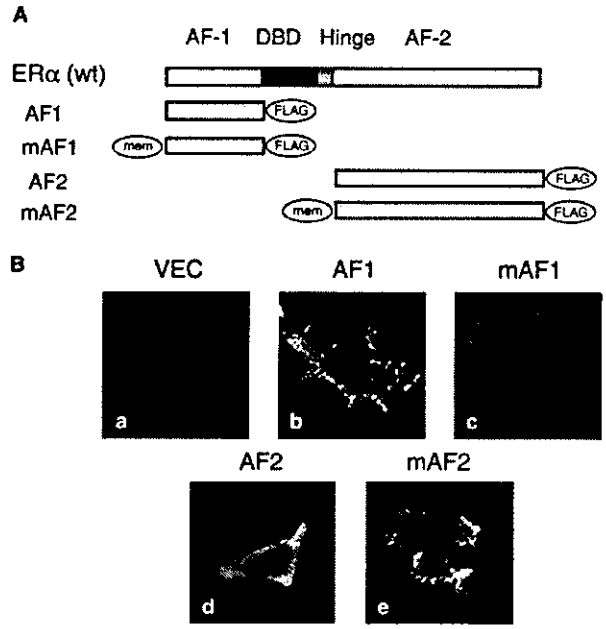

Fig. 1. Establishment of cell lines stably expressing a series of domain fragments of Erα in MCF-7. (A) Schematic representation of wild-type full-length ERα (wt), FLAG epitope-tagged AF-1 domain constructs with and without the membrane-targeting sequence (mem), and FLAG epitope-tagged AF-2 domain constructs with or without the membrane-targeting sequence. (B) Stable transfectants were immunostained with anti-FLAG antibody. (a) Empty vector; (b) AF1; (c) mAF1; (d) AF2; (e) mAF2. Cells were visualized with a confocal microscope at a magnification of 600×.

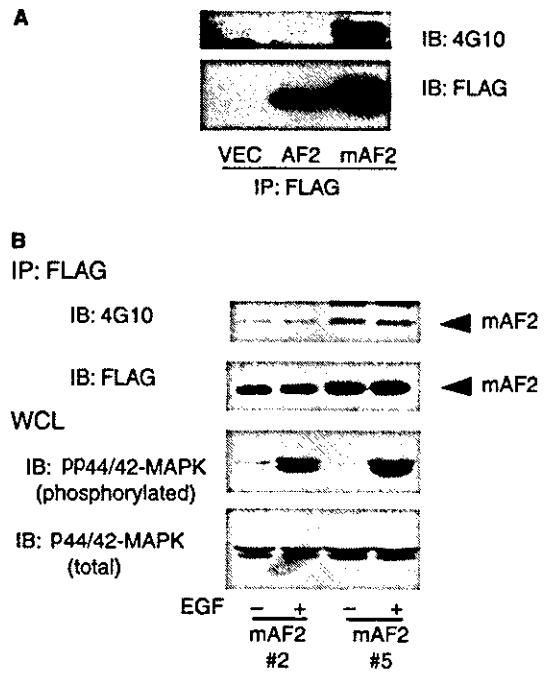

Fig. 2. Tyrosine phosphorylation of AF-2 domain at the plasma membrane. (A) Cell lysates of AF2 and mAF2 were immunoprecipitated with anti-FLAG antibody. Cells transfected with an empty vector (VEC) were used as a negative control. Each immunoprecipitate was subjected to immunoblotting analysis with anti-phosphotyrosine antibody 4G10 and anti-FLAG antibody. (B) Two independent clones of mAF2 (clones #2 and #5) were treated with either EGF (100 ng/ml) or distilled water for 5 min. mAF2 fragments were immunoprecipitated with anti-FLAG antibody and immunoblotted for 4G10 and anti-FLAG antibody. Whole cell lysates (WCLs) were immunoblotted with anti-phosphorylated p44/42 MAPK antibody and anti-p44/42 MAPK antibody.

zation using the stable transfectants we had established. The tyrosine phosphorylation of the mAF2 domain fragment was observed using phosphotyrosine specific antibody; however, almost no phosphorylation was detected in AF2 (Fig. 2A). This indicates that the AF-2 domain is phosphorylated exclusively at the plasma membrane.

To further characterize the tyrosine phosphorylation of the AF-2 domain, two independent clones of mAF2 cells were stimulated by EGF. In breast cancer cells, several tyrosine kinases, such as src family kinases [18,19] and Her-2 [20], have been reported to be transactivated upon EGF stimulation. However, no remarkable difference in the level of phosphorylation of mAF2 was observed upon EGF stimulation (Fig. 2B), suggesting that ERα is not the substrate of tyrosine kinases that is activated by EGF stimulation.

3.3. *Screening of the membrane-specific binding partners of the AF-1 and AF-2 domains*

In order to identify the interacting molecules with each domain of ERα, the lysates of the stable transfectants were purified with the anti-FLAG immunoaffinity column and analyzed by subsequent silver staining. Several candidates for mAF1-associated proteins were visualized by these procedures (Fig. 3). The bands around 200 kDa (arrowhead a), 50 kDa (arrowhead c) and 40 kDa (arrowhead d) were specifically seen in cells expressing mAF1, while the band around 70 kDa (arrowhead b) was observed in both cells expressing AF1 and cells expressing mAF1. None of these bands was co-purified with mAF2. These four bands were visible in the CBB gel stain from large-scale sample preparation. Two of these were successfully identified by LC/MS/MS analysis. The 50-kDa band that was specific to membrane-targeted AF1 was identified as β-tubulin (arrowhead c in Fig. 3). The 70-kDa band which was seen in both AF1 and mAF1 but not in mAF2 was identified as heat shock protein 70 (Hsp70) (arrowhead b in Fig. 3). Proteins specifically bound to mAF2 were not detected by this protocol (Fig. 3), although larger-scale purification was further attempted.

The association of mAF1 with β-tubulin was confirmed by immunoprecipitation followed by detection with β-tubulin antibody (Fig. 4A). This association was not detected in cells expressing AF1, indicating that this association is localized only at the plasma membrane. The absence of association between mAF2 and β-tubulin suggests that the association with β-tubulin was AF-1 domain-dependent and the membrane-targeting sequence did not serve as binding site for β-tubulin. A similar manner of association between mAF1 and α-tubulin was also detected (Fig. 4A), which is supported by the fact that β-tubulin forms heterodimers with α-tubulin.

To investigate physiological cooperation of tubulin and full-length endogenous ERα, immunocytostaining of MCF-7 cells was performed (Fig. 4B). Estrogen-dependent translocation of ERα to the plasma membrane was observed in 15 min on estrogen stimulation (Fig. 4B: h and k). At the same time, redistribution of α-tubulin was also observed at the plasma membrane (Fig. 4B: g and j). These two molecules showed co-localization in the superimposed image (Fig. 4B: i and l), which indicates possible association of these molecules in intact

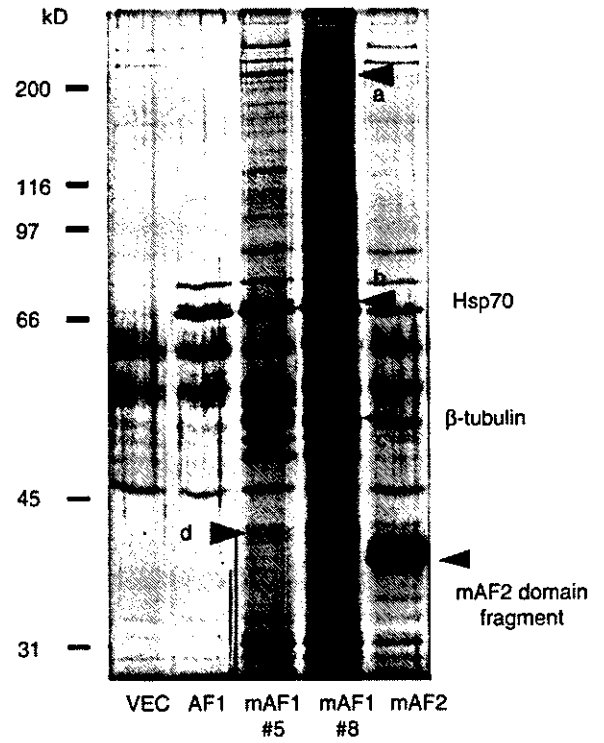

Fig. 3. Associated molecules to each domain fragment of ERα detected by silver staining. Each FLAG epitope-tagged domain fragment was immunoprecipitated by anti-FLAG antibody. One AF1 clone, two independent mAF1 clones (clones #5 and #8), and one mAF2 clone were analyzed. Immunoprecipitates were subjected to SDS–PAGE, and the gel was silver-stained. The two bands indicated by the arrowheads are Hsp70 and β-tubulin, which were identified later by LC/MS/MS analysis.

MCF-7 cells. These phenomena were not observed in the cells treated only by ethanol (Fig. 4B: d–f).

To further characterize the association of mAF1 and tubulins, cells expressing AF1 or mAF1 were treated with nocodazole, an inhibitor of tubulin polymerization. As a result, nocodazole treatment significantly blocked the association of mAF1 and α-tubulin (Fig. 4C). This indicates that mAF1 has higher affinity with polymerized microtubule filaments than with the depolymerized heterodimeric tubulin subunit.

Hsp70 was immunoprecipitated with both the AF1 and mAF1 domain fragments, but not with mAF2 (Fig. 4D). This suggests that the AF-1 domain is associated with Hsp70 outside the nucleus, but this association is not a membrane-specific event, in contrast with the case of tubulin.

4. Discussion

This study identifies polymerized tubulins as specific binding partners of the AF-1 domain of ERα at the plasma membrane using a breast cancer cell line, MCF-7. Hsp70 was also found to associate with the AF-1 domain although this association is not restricted at the plasma membrane. It was demonstrated that tyrosine phosphorylation of the AF-2 domain occurred within the plasma membrane, while the membrane-localized AF-2 domain failed to characterize any significant binding partners.

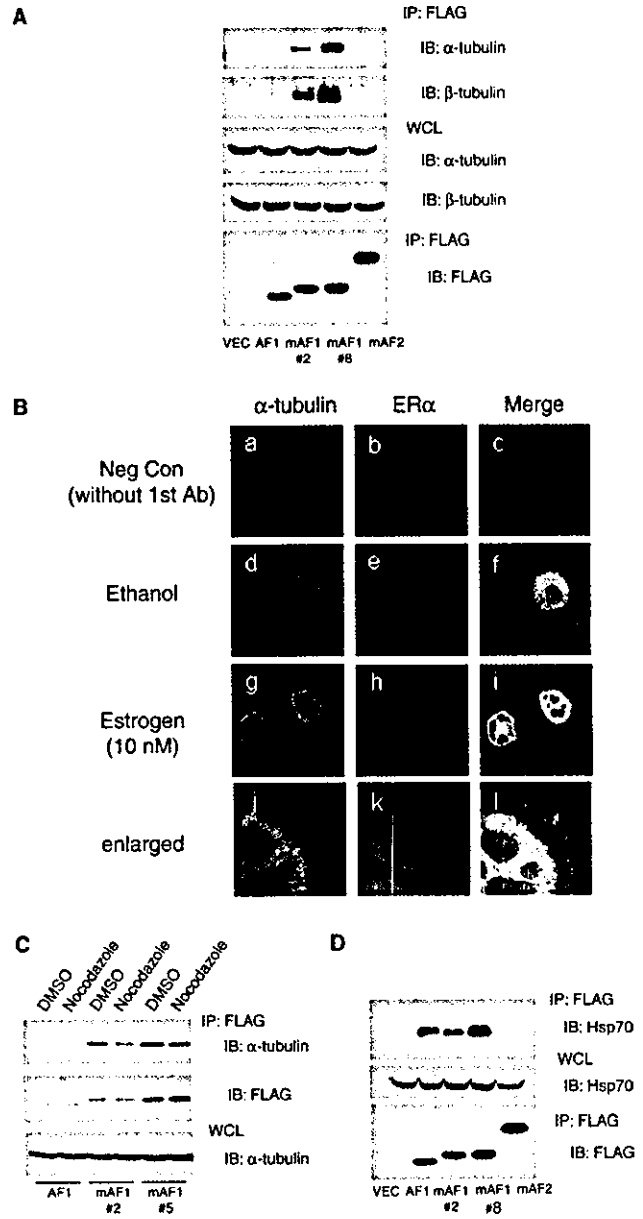

Fig. 4. Association of tubulins and Hsp70 with the AF-1 domain of ERα. (A) Cell lysates were immunoprecipitated and immunoblotted with anti-FLAG antibody, or anti-α- or β-tubulin antibodies as indicated. One AF1 clone, two independent mAF1 clones (clones #2 and #8), and one mAF2 clone were analyzed. (B) MCF-7 cells were treated with estrogen (10 nM) or ethanol (same concentration used in dilution of estrogen) for 15 min, then they were immunostained with anti-α-tubulin antibody (a, d, g, and j: green), and anti-ERα antibody (b, e, h, and k: red). Cells were visualized with a confocal microscope at a magnification of 600×. Superimposed confocal images (c, f, i, and l: merge) are also shown. Images without first antibodies (a–c) are shown as negative controls. Membranous area of estrogen stimulated MCF-7 cells was shown in magnified views (j–l: enlarged). (C) One AF1 clone and two independent mAF1 clones (clones #2 and #5) were treated with Nocodazole (33-μmol solution in DMSO) or DMSO (negative control) for 1 h. Cell lysates were immunoprecipitated and immunoblotted as indicated. (D) Cell lysates were immunoprecipitated and immunoblotted with anti-FLAG or anti-Hsp70 antibodies as indicated. One AF1 clone, two independent mAF1 clones (clones #2 and #8), and one mAF2 clone were analyzed.

It has been suggested by several independent laboratories that a subpopulation of ERα is associated with the plasma membrane and is responsible for the rapid effects of estrogen [15,16]. However, it appears that the subpopulation of membrane-associated ERα is considerably small, while the majority of ERα translocates into the nucleus upon estrogen stimulation. Therefore, we targeted the AF-1 and AF-2 domains of ERα to the plasma membrane to overcome the small amount of endogenous receptors at the plasma membrane.

The association of the AF-1 domain with polymerized tubulins or microtubules was specifically detected with the membrane-localized type of AF1, despite the wide distribution of microtubules throughout the cytoplasm. This result led us to conjecture that the association of ERα and microtubules is mediated by other molecules that reside at the membrane. Some signaling molecules are reported to associate with microtubules at the plasma membrane. p190RhoGEF (guanine nucleotide exchange factor) has a PH (pleckstrin homology) domain and localizes at the plasma membrane. This RhoA-activating molecule, which affects transcription and actin reorganization, has also been shown to interact directly with microtubules [21]. A small GTPase K-Ras, which can transduce signals to Erk, is another molecule shown to associate with microtubules at the plasma membrane [22]. It is possible that ERα forms a complex with K-Ras, microtubules and other unidentified molecules and affects the Ras signaling pathway. This may explain the rapid elevation of phosphorylated Erk on estrogen stimulation. The anti-tumor drug, paclitaxel, which is often used in the treatment. of breast cancer, has been shown to associate with polymerized microtubules and affect Ras-dependent signaling events [23]. This suggests that paclitaxel might also function by dissociating the signaling complex that involves ERα, K-Ras, and microtubules.

Association between the AF-1 domain and microtubules also tells us that microtubules are not used as tracks when ERα is transported to the plasma membrane, because the AF-1 domain needs to associate with microtubules at the cytoplasm before translocation if microtubules are used as tracks. Although membrane translocation is an important step for the non-genomic action of ERα, the precise mechanism is still elusive.

Ligand-dependent redistribution of both tubulins and ERα toward plasma membrane strongly suggests physical association between these molecules. To show the interaction of full-length ERα and tubulins, immunoprecipitation of tubulins or ERα was attempted several times using MCF-7 and Cos-7 cells. However, no association between tubulins and endogenous ERα was observed (data not shown). Immunocytostaining revealed that most of the full-length ERα was expressed in the nucleus and this situation was not improved even when membrane localizing sequence was attached to full-length ERα. Therefore, we concluded that our antibodies are not sensitive enough to detect the small population of membrane-localizing full-length ERα by immunoprecipitation.

It remains to be elucidated whether translocation of the small part of tubulins is a consequence of ERα translocation or an independent event. Nevertheless, this observation may indicate biological cooperation between ERα and tubulins.

It is also possible that the association of ERα and tubulins might contribute to the stabilization of microtubules, since mAF1 has higher affinity with polymerized tubulin and tubulin was well visualized at the plasma membrane when ERα was co-localized.

Hsp70 was shown to be another molecule that associates with the AF-1 domain expressed outside the nucleus. This association was not restricted at the membrane. The physiological role of the association between the AF-1 domain and Hsp70 is unclear. One possibility is that this association is involved in the degradation of cytoplasmic ERα. The glucocorticoid receptor, another member of the nuclear receptor superfamily, is shown to associate with Hsp90. CHIP, a U-box protein that has ubiquitin ligase activity, was shown to interact directly with Hsp90 and promote the degradation of glucocorticoid receptor [24]. CHIP was originally found as a Hsp70 interacting protein, and is also shown to localize outside the nucleus and to promote the degradation of Hsp70 bound protein [25]. Therefore, it is conceivable that in the case of ERα, Hsp70 mediates the degradation of cytoplasmic population of ERα. The degradation of ERα inside the nucleus was shown to be regulated differently depending on whether ERα is liganded or unliganded, and this mode of degradation generates a cyclic rhythm in the recruitment of ERα on estrogen-responsive promoters [26]. Hsp70 may be involved in the different regulation of ERα turnover outside the nucleus, which reflects the different functions of ERα outside the nucleus.

We also showed that tyrosine phosphorylation of the AF-2 domain occurs at the plasma membrane. It was previously reported that the AF-2 domain of ERα is phosphorylated on estrogen stimulation [15]. However, it was not clear whether the AF-2 domain is phosphorylated before or after membrane translocation. Our results favor the latter scenario. As the AF-2 domain without the membrane-targeted signal was not phosphorylated, the tyrosine kinases responsible for AF-2 phosphorylation localize strictly in the membranous area. Therefore, we assume that AF-2 phosphorylation does not regulate membrane translocation itself and that estrogen stimulation elicits the membrane translocation of ERα through interaction independent of phosphotyrosine.

So, what is the role of tyrosine phosphorylation of the AF-2 domain at the plasma membrane? Does phosphotyrosine mediate specific signals when the receptor translocates to the plasma membrane? Despite several attempts at purification, we have not yet identified the AF2-associated proteins. One of the factors that prevented the identification of the associated proteins was that the tyrosine-phosphorylated population of the AF-2 domain fragment was extremely small. The phosphorylation of the membrane-localized AF-2 domain was hardly detected by transient transfectants (data not shown). We managed to detect tyrosine phosphorylation of the membrane-localized AF-2 domain using stable transfectants. As long as the phosphorylated population of the membrane-localized AF-2 domain is small, only a small amount of molecules is supposed to bind to the AF-2 domain in a phosphotyrosine-dependent manner. This may be the reason that the previously reported association of membrane-localized AF-2 and c-Src [15] was not detected using our method (data not shown). Another possible factor that prevented the identification of the associated proteins is that AF-2 domain-bound proteins require the other domains of ERα to stabilize their association. In this case, longer ERα constructs would be needed to purify AF-2-associated proteins.

However, this is technically difficult because strong nuclear localization signals in the DBD and hinge region prevent the membrane localization of longer constructs, even though the membrane-targeting signal was attached to them (data not shown).

Another limitation of this purification method was that only proteins existing abundantly in the cytoplasm, such as tubulins and Hsp70, were identified as AF-1 domain-associated proteins. It is possible that signaling molecules, which are not expressed abundantly enough to be detected using our method, interact with the AF-1 or AF-2 domain at the plasma membrane and play an important role. Further improvement in our purification and identification method is necessary to characterize these molecules.

In conclusion, we have shown that the AF-1 domain of ERα interacts with microtubules at the plasma membrane, and Hsp70 outside the nucleus. We also demonstrated that the AF-2 domain of ERα is phosphorylated at the plasma membrane. We hypothesize that ERα forms a complex with microtubule-associated signaling molecules and phosphotyrosine-dependent AF-2-associated molecules. However, the whole view of the ERα complex is still unclear. To understand the pathological function of ERα in breast cancers, further investigation is required. This will lead to further improvement in breast cancer therapy and also bring about a deeper understanding of the physiological processes in which nuclear receptors are involved.

Acknowledgements: We thank Dr. I. Kitabayashi (Molecular Oncology Division, National Cancer Center Research Institute) for mass spectrometry analysis. K.A. is an awardee of the Research Resident Fellowship from the Foundation for Promoting Cancer Research (Japan) for the third Term Comprehensive 10-Year Strategy for Cancer Control. This study was supported by the Program for the Promotion of Fundamental Studies in the Health Science of Pharmaceuticals and Medical Devices Agency (PMDA).

References

[1] Evans, R.M. (1988) Science 240, 889–895.
[2] Mangelsdorf, D.J. et al. (1995) Cell 83, 835–839.
[3] Tora, L., White, J., Brou, C., Tasset, D., Webster, N., Scheer, E. and Chambon, P. (1989) Cell 59, 477–487.
[4] Endoh, H. et al. (1999) Mol. Cell. Biol. 19, 5363–5372.
[5] Rachez, C. et al. (1999) Nature 398, 824–828.
[6] Watanabe, M. et al. (2001) EMBO J. 20, 1341–1352.
[7] Belandia, B., Orford, R.L., Hurst, H.C. and Parker, M.G. (2002) EMBO J. 21, 4094–4103.
[8] Yanagisawa, J. et al. (2002) Mol. Cell. 9, 553–562.
[9] Belandia, B. and Parker, M.G. (2003) Cell 114, 277–280.
[10] Fernandes, I. et al. (2003) Mol. Cell. 11, 139–150.
[11] Ylikomi, T., Bocquel, M.T., Berry, M., Gronemeyer, H. and Chambon, P. (1992) EMBO J. 11, 3681–3694.
[12] Haynes, M.P., Sinha, D., Russell, K.S., Collinge, M., Fulton, D., Morales-Ruiz, M., Sessa, W.C. and Bender, J.R. (2000) Circ. Res. 87, 677–682.
[13] Simoncini, T., Hafezi-Moghadam, A., Brazil, D.P., Ley, K., Chin, W.W. and Liao, J.K. (2000) Nature 407, 538–541.
[14] Kousteni, S. et al. (2001) Cell 104, 719–730.
[15] Migliaccio, A. et al. (2000) EMBO J. 19, 5406–5417.
[16] Song, R.X., McPherson, R.A., Adam, L., Bao, Y., Shupnik, M., Kumar, R. and Santen, R.J. (2002) Mol. Endocrinol. 16, 116–127.
[17] Hochstrasser, D.F., Patchornik, A. and Merril, C.R. (1988) Anal. Biochem. 173, 412–423.
[18] Osherov, N. and Levitzki, A. (1994) Eur. J. Biochem. 225, 1047–1053.
[19] Luttrell, D.K. et al. (1994) Proc. Natl. Acad. Sci. USA 91, 83–87.
[20] Muthuswamy, S.K. and Muller, W.J. (1995) Oncogene 11, 271–279.
[21] van Horck, F.P., Ahmadian, M.R., Haeusler, L.C., Moolenaar, W.H. and Kranenburg, O. (2001) J. Biol. Chem. 276, 4948–4956.
[22] Chen, Z., Otto, J.C., Bergo, M.O., Young, S.G. and Casey, P.J. (2000) J. Biol. Chem. 275, 41251–41257.
[23] Wang, T.H., Popp, D.M., Wang, H.S., Saitoh, M., Mural, J.G, Henley, D.C., Ichijo, H. and Wimalasena, J. (1999) J. Biol. Chem. 274, 8208–8216.
[24] Connell, P., Ballinger, C.A., Jiang, J., Wu, Y., Thompson, L.J., Hohfeld, J. and Patterson, C. (2001) Nat. Cell. Biol. 3, 93–96.
[25] Meacham, G.C., Patterson, C., Zhang, W., Younger, J.M. and Cyr, D.M. (2001) Nat. Cell. Biol. 3, 100–105.
[26] Reid, G. et al. (2003) Mol. Cell. 11, 695–707.

Behavioral/Systems/Cognitive

Hippocampal Synaptic Modulation by the Phosphotyrosine Adapter Protein ShcC/N-Shc via Interaction with the NMDA Receptor

Yoshiaki Miyamoto,[1] Ling Chen,[2] Masahiro Sato,[1] Masahiro Sokabe,[2,3] Toshitaka Nabeshima,[4] Tony Pawson,[5] Ryuichi Sakai,[6] and Nozomu Mori[1,7]

[1]Department of Molecular Genetics, National Institute for Longevity Sciences, Oobu 474-8522, Japan, [2]Cell Mechanosensing Project, International Cooperative Research Project–Japan Science and Technology Agency, and Departments of [3]Physiology and [4]Neuropsychopharmacology and Hospital Pharmacy, Nagoya University Graduate School of Medicine, Nagoya 466-8560, Japan, [5]Department of Molecular and Medical Genetics, University of Toronto, Toronto, Ontario M5S 1A8, Canada, [6]Growth Factor Division, National Cancer Center Research Institute, Tokyo 104-0045, Japan, and [7]Department of Anatomy and Neurobiology, Nagasaki University School of Medicine, Nagasaki 852-8523, Japan

N-Shc (neural Shc) (also ShcC), an adapter protein possessing two phosphotyrosine binding motifs [PTB (phosphotyrosine binding) and SH2 (Src homology 2) domains], is predominantly expressed in mature neurons of the CNS and transmits neurotrophin signals from the TrkB receptor to the Ras/mitogen-activated protein kinase (MAPK) pathway, leading to cellular growth, differentiation, or survival. Here, we demonstrate a novel role of ShcC, the modulation of NMDA receptor function in the hippocampus, using *ShcC* gene-deficient mice. In behavioral analyses such as the Morris water maze, contextual fear conditioning, and novel object recognition tasks, ShcC mutant mice exhibited superior ability in hippocampus-dependent spatial and nonspatial learning and memory. Consistent with this finding, electrophysiological analyses revealed that hippocampal long-term potentiation in ShcC mutant mice was significantly enhanced, with no alteration of presynaptic function, and the effect of an NMDA receptor antagonist on its expression in the mutant mice was notably attenuated. The tyrosine phosphorylation of NMDA receptor subunits NR2A and NR2B was also increased, suggesting that ShcC mutant mice have enhanced NMDA receptor function in the hippocampus. These results indicate that ShcC not only mediates TrkB-Ras/MAPK signaling but also is involved in the regulation of NMDA receptor function in the hippocampus via interaction with phosphotyrosine residues on the receptor subunits and serves as a modulator of hippocampal synaptic plasticity underlying learning and memory.

Key words: ShcC/N-Shc; phosphotyrosine adapter protein; learning and memory; long-term potentiation; hippocampus; NMDA receptor

Introduction

Long-term potentiation (LTP) in the hippocampus, a well characterized form of activity-dependent synaptic plasticity, serves as a major cellular mechanism of learning and memory (Bliss and Collingridge, 1993; Malenka and Nicoll, 1999). The NMDA and AMPA types of glutamate receptors (GluRs) play critical roles in the induction of hippocampal LTP (Tsien et al., 1996; Zamanillo et al., 1999). In addition to the primary importance of the glutamate receptors, it has been reported that neurotrophins, particularly brain-derived neurotrophic factor (BDNF), modulate the maintenance of hippocampal LTP through the activation of TrkB receptor tyrosine kinases (Poo, 2001; Lu, 2003). Also, a variety of intracellular signaling cascades, including the Ras/mitogen-activated protein kinase (MAPK) pathway, are reported to influence LTP formation (Ohno et al., 2001; Silva, 2003).

The BDNF-activated TrkB receptors recruit various adapter proteins such as Shc, Frs-2, and phospholipase-Cγ (PLCγ). The adapter proteins are tyrosine phosphorylated by the activated TrkB receptors and determine the flow of downstream intracellular signaling cascades to cellular growth, differentiation, or survival. Binding of Shc or Frs-2 leads to the activation of Ras/MAPK and PI3K (phosphoinositide-3 kinase)/Akt pathways, whereas binding of PLCγ stimulates the release of intracellular Ca^{2+} via inositol 1,4,5-trisphosphate (IP3) and thereby activates the Ca^{2+}–calmodulin-dependent kinase IV (CaMKIV) pathway (Kaplan and Miller, 2000; Patapoutian and Reichardt, 2001). Therefore, it is hypothesized that TrkB-Ras/MAPK signaling plays a role in the hippocampal LTP underlying learning and memory (Adams and Sweatt, 2002; Ying et al., 2002).

The Shc family consists of ShcA/Shc (p66, p52, and p46 isoforms), ShcB/Sck (p68), and ShcC/neural Shc (N-Shc) (p69 and p55), and possesses two modular regions that bind to phosphorylated tyrosine-containing peptide motifs: a PTB (phosphoty-

Received March 3, 2004; revised Dec. 30, 2004; accepted Jan. 3, 2005.

The initial part of this work was supported by the program "Protecting the Brain" of the Core Research for Evolutional Science and Technology–Japan Science and Technology Agency, and later, in part, by a Virtual Research Institute of Aging fund of Nippon Boehringer Ingelheim, the Uehara Memorial Research Fund, Funds for Comprehensive Research on Aging and Health from Ministry of Health, Labor, and Welfare, and grants-in-aid from the Ministry of Education, Culture, Sports, Science, and Technology of Japan. We thank Dr. T. Nakamura for valuable advice and I. Nakano and Y. Kadokawa for technical assistance and laboratory maintenance.

Correspondence should be addressed to Dr. Nozomu Mori, Department of Anatomy and Neurobiology, Nagasaki University School of Medicine, 1-12-4 Sakamoto, Nagasaki 852-8523, Japan. E-mail: morinosm@net.nagasaki-u.ac.jp.

DOI:10.1523/JNEUROSCI.3030-04.2005

 0270-6474/05/251826-10$15.00/0

rosine binding) domain and an SH2 (Src homology 2) domain. All of the Shc family members serve to link a number of receptor tyrosine kinases with multiple intracellular signaling cascades. ShcA is widely expressed in most tissues, whereas both ShcB and ShcC are predominantly expressed in the nervous system (Cattaneo and Pelicci, 1998; Ravichandran, 2001). The brain-enriched ShcC would be in a good position to modulate the hippocampal LTP via regulation of TrkB-Ras/MAPK signaling, because it has been implicated in the BDNF-TrkB signaling toward the Ras/MAPK pathway in cultured cells (Nakamura et al., 1998; Liu and Meakin, 2002).

Recent studies revealed that the so-called "Shc site" of the TrkB receptor (Tyr^{515}) was not relevant to the hippocampal LTP, because mice with a targeted point mutation of the TrkB–Shc site showed apparently no significant change in LTP formation (Korte et al., 2000; Minichiello et al., 2002). These findings are in contrast to the aforementioned hypothesis pointing to a role for TrkB-Ras/MAPK signaling in the hippocampal LTP. Accordingly, in the present study, we attempted to clarify whether the phosphotyrosine adapter protein *ShcC*, which binds the TrkB–Shc site leading to the Ras/MAPK pathway, is involved in hippocampal functions, using *ShcC* gene-deficient mice. Based on the results presented herein, we propose a novel role for ShcC in hippocampal synaptic plasticity, as evidenced by the enhancement of hippocampal LTP and hippocampus-dependent learning and memory in ShcC mutant mice.

Materials and Methods

Animals. Mice lacking ShcC were generated by Sakai et al. (2000). The homozygous mutant mice (−/−; 3 months of age) and the littermate 2 wild-type mice (+/+; 3 months of age) were obtained by crossing F2 heterozygous mutant mice (+/−). The genotypes of mice were determined by Southern blot analyses of tail DNA. C57BL/6 mice (Nihon SLC, Hamamatsu, Japan) were used for biochemical analyses of the Shc family members. The mice were housed in plastic cages and were kept in a regulated environment (24 ± 1°C; 50 ± 5% humidity), with a 12 h light/dark cycle (lights on at 9:00 A.M.). Food and tap water were available *ad libitum*. All of the experiments were performed in accordance with the Guidelines for Animal Experiments of the Nagoya University School of Medicine. The procedures involving animals and their care were conducted in conformity with the international guidelines *Principles of Laboratory Animal Care* (National Institutes of Health publication 85-23, revised 1985).

Plasmids and antibodies. Plasmids encoding cDNAs of mouse p52-ShcA, p68-ShcB, and p55-ShcC were as described previously (Kojima et al., 2001) and were epitope-tagged with T7 at the N terminus. Antibodies against ShcA (catalog #S68020) and ShcC (S55720) were obtained from Transduction Laboratories (San Diego, CA). Antibody against ShcB was prepared as described previously (Sakai et al., 2000). Anti-phosphotyrosine antibody (catalog #05-321) was purchased from Upstate Biotechnology (Charlottesville, VA). Antibodies against NR1 (catalog #sc-9058), NR2A (catalog #sc-9056), NR2B (catalog #sc-9057), postsynaptic density 95 (PSD95) (catalog #sc-6926), Src (catalog #sc-5266), Fyn (catalog #sc-434), and the Src family (catalog #sc-18) were from Santa Cruz Biotechnology (Santa Cruz, CA). Anti-phospho-Src family (Tyr^{418}) antibody (catalog #44-660) was purchased from Biosource (Camarillo, CA).

Northern blot analysis. Total RNAs were isolated using TRIzol reagents (Invitrogen, Carlsbad, CA). Isolated total RNAs (20 μg) were electrophoresed on a formalin/agarose gel and blotted onto a positively charged nylon membrane. Specific cDNA probes for the Shc family members were made by Megaprime DNA labeling systems and [α-^{32}P]dCTP (Amersham Biosciences, Piscataway, NJ) and purified with NucTrap Probe Purification Columns (Stratagene, La Jolla, CA). Membranes were hybridized with the ^{32}P-labeled cDNA probes as described previously (Nakamura et al., 1998).

In situ *hybridization analysis.* Mouse brain sections (15 μm) were cut on a cryostat, thaw-mounted on poly-L-lysine-coated slides, and stored at −80°C until use. The frozen brain sections were brought to room temperature and air-dried. The sections were postfixed with 4% paraformaldehyde in 0.1 M phosphate buffer, acetylated with 0.25% acetic anhydride in 0.1 M triethanolamine, and dehydrated through an ascending series of ethanol concentrations. To prepare antisense and sense cRNA probes, the plasmids encoding cDNA of ShcA, ShcB, or ShcC were linearized by cutting at a single site (antisense, *Eco*RI; sense, *Hin*dIII). *In vitro* transcription was performed using RNA polymerase (antisense, T7 RNA polymerase; sense, SP6 RNA polymerase) and [α-^{35}S]UTP (ICN Biomedicals, Costa Mesa, CA). *In situ* hybridization with the ^{35}S-labeled cRNA probes was performed as described previously (Nakamura et al., 1998). The sections were counterstained with thionine and dehydrated. The images were captured by the HC-2000 video camera system (Fuji Photo Film, Tokyo, Japan) and reconstructed using computer software.

Western blot analysis and immunoprecipitation assay. Mouse brains were homogenized in a lysis buffer [50 mM Tris-HCl, pH 7.5, 150 mM NaCl, 5 mM EDTA, 10 mM NaF, 1 mM sodium orthovanadate, 1% Triton X-100, 0.5% sodium deoxycholate, 1 mM phenylmethylsulfonyl fluoride, and protease inhibitor mixture (Complete; Roche, Mannheim, Germany)] or a modified lysis buffer containing 0.1% SDS for immunoprecipitation assays. For Western blot analysis, total proteins (10 μg) were separated by SDS-PAGE and blotted onto a polyvinylidene difluoride (PVDF) membrane. For immunoprecipitation assays, total proteins (500 μg) were incubated with an appropriate antibody and then protein G-Sepharose was added and further incubated. The immunoprecipitates were recovered by centrifugation and resuspended in a sample buffer. The samples (10 μl) were separated by electrophoresis and blotted onto a PVDF membrane. The membranes were incubated with primary antibodies, and proteins were detected by HRP-conjugated secondary antibodies using the ECL detection kit (Amersham Biosciences).

Histological analysis. Mouse brains were perfused with 4% paraformaldehyde in PBS and removed. Sections (15 μm) were cut, mounted on slides, and stored at −80°C until use. Nissl staining was done according to standard procedures. The images were captured with an HC-2000 video camera system. For immunochemical staining, the sections were permeabilized with 0.2% Triton X-100, blocked with 3% BSA, and incubated with antibody against microtubule-associated protein 2 (MAP2) (catalog #M1406; Sigma, St. Louis, MO). To detect specific signals for MAP2, the sections were incubated with Alexa Fluor 488-conjugated secondary antibody (catalog #A-11029; Molecular Probes, Eugene, OR). Fluorescence images were obtained with the confocal imaging system Micro Radiance (Bio-Rad Laboratories, Hercules, CA).

Behavioral analysis. To measure locomotor activity, a mouse was placed in a transparent acrylic cage with a black Plexiglas floor (45 × 26 × 40 cm), and locomotion and rearing were measured for 60 min using infrared counters (Scanet SV-10; Toyo Sangyo, Toyama, Japan).

To measure nociceptive responses to electric footshock, a mouse was placed in a transparent Plexiglas cage with a grid floor for footshock (25 × 30 × 11 cm) and an ascending footshock series (0.01, 0.02, 0.03, 0.04, 0.05, 0.06, 0.08, 0.10, 0.13, 0.16, 0.20, 0.25, 0.30, 0.40, 0.50, and 0.60 mA for 0.5 s; 30 s interval) was delivered through an electric shock generator (NS-SG01; Neuroscience, Tokyo, Japan). The electric current needed to elicit first flinching, vocalizing, or jumping behavior was recorded as the footshock threshold.

For the Morris water maze task, a pool (120 cm in diameter) was prepared with white plastic, and the water temperature was maintained at 20°C. Swimming paths were analyzed by a computer system with a video camera (AXIS-90 Target/2; Neuroscience). In the hidden-platform test, the platform (7 cm in diameter) was submerged 1 cm below the water surface. Mice did not swim in the pool before training. Three starting positions were used pseudorandomly, and each mouse was trained with three trials per day for 6 d. After reaching the platform, the mouse was allowed to remain on it for 30 s. If the mouse did not find the platform within 60 s, the trial was terminated and the animal was put on the platform for 30 s. In the platform transfer test, the mouse swam for 60 s in the pool without the platform. In the visible-platform test, the black platform was located 1 cm above the water surface.

For the fear conditioning task, a mouse was placed in a training cage

(25 × 30 × 11 cm), which consisted of transparent Plexiglas with a grid floor for footshock, and the freezing response as the immobility time was measured for 2 min in the absence of sound and footshock (preconditioning) using Scanet SV-10AQ (Toyo Sangyo), which can measure automatically the immobility time by digital counters with infrared sensors. In the conditioning, the mouse was again placed in the cage, and the pretrial time of 2 min was followed by a 15 s tone stimulus (80 dB). During the last 5 s of the tone stimulus, a footshock of 0.8 mA was delivered through a shock generator (NS-SG01; Neuroscience). This procedure was repeated four times with 15 s intervals. In the pseudoconditioning, the mouse was exposed to the conditioning without footshock. For the contextual test 24 h after the conditioning, the mouse was placed back in the same cage in the absence of sound and footshock. For the cued test 24 h after the conditioning, the mouse was placed in a novel cage (45 × 26 × 40 cm), which was made of a transparent acrylic cage with a black Plexiglas floor, in the presence of a continuous tone stimulus.

For the novel object recognition task, a mouse was habituated to a black plastic cage (30 × 30 × 50 cm) for 3 d. In the training, two novel objects were placed in the cage, and the mouse was allowed to explore freely for 5 min. Time spent exploring each object was recorded manually. In retentions 2 or 24 h after the training, the mouse was placed back in the same cage, in which one of the familiar objects used in the training was replaced by a novel object, and allowed to explore for 5 min. Exploratory preference, a ratio of time spent exploring any one of the two objects (training) or the novel one (retention) over the total time spent exploring both objects, was used to measure recognition memory.

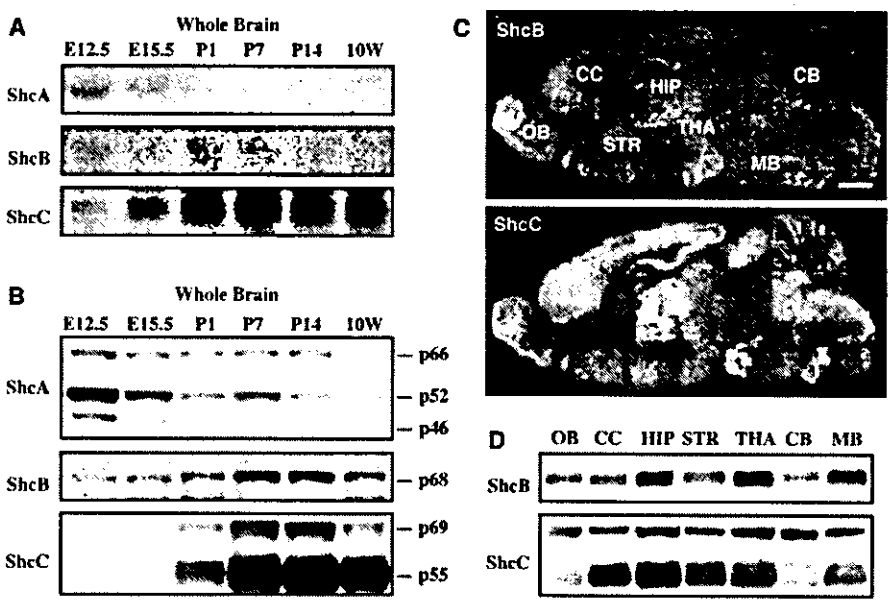

Figure 1. Expression profiles of Shc family members in the brain. *A*, mRNA expression of Shc family members during brain development. Total RNAs from whole brain in various developmental stages were examined by Northern blot analysis. *B*, Protein expression of Shc family members during brain development. Protein extracts from whole brain in various developmental stages were examined by Western blot analysis. *C*, mRNA expression of ShcB and ShcC in the mature brain [10 weeks of age (10W)]. mRNAs were examined by *in situ* hybridization analysis. Scale bar, 1 mm. *D*, Protein expression of ShcB and ShcC in various regions of the mature brain (10W). Protein extracts from various regions of the brain were examined by Western blot analysis. E12.5 and E15.5, Embryonic days 12.5 and 15.5; OB, olfactory bulb; CC, cerebral cortex; HIP, hippocampus; STR, striatum; THA, thalamus; CB, cerebellum; MB, midbrain.

Electrophysiological analysis. Mouse brains were removed and kept in artificial CSF (ACSF) (in mM: 128 NaCl, 1.7 KCl, 26 $NaHCO_3$, 1.2 KH_2PO_4, 2.4 $CaCl_2$, 1.3 $MgSO_4$, and 10 glucose). ACSF was saturated with a mixture of 95% O_2/5% CO_2. Slices of the hippocampus (350 μm) were prepared using a microslicer (DTK-1500; Dosaka EM, Kyoto, Japan) and placed for 1 h in an incubation chamber filled with ACSF. The slices were stained with a voltage-sensitive dye, RH 482 (0.1 mg/ml; Nippon Kanko-Shikiso Kenkyusho, Okayama, Japan). The stained slices were transferred to a recording chamber mounted on an inverted microscope (IMT-2; Olympus, Tokyo, Japan). The recording chamber was continuously perfused with ACSF. The optical recording system (HR Deltaron 1700; Fuji Photo Film) consists of an area sensor with 128 × 128 photodiodes and a data-processing unit. Each photodiode receives optical signals from a 25 × 25 μm sample area, thus creating a 3.3 × 3.3 mm recording field. For optical recordings, an ACSF-filled glass electrode was placed in the hippocampal CA3 area. Schaffer collateral afferents were then stimulated with 300 μA/200 μs pulses, and a test stimulus was delivered at 0.06 Hz by a stimulator (SEN-3301; Nihon Kohden, Tokyo, Japan). In each trial, background signals were recorded for 10 ms before the electrical stimulus and stored as a reference image. Images after the stimulus were recorded at 0.6 ms/frame, and the difference signals from the reference image were digitized into 8 bit signals. The digitized signals were then amplified 400 times. To improve the signal-to-noise ratio, 16 trial images were averaged into a single image. A total of 150 sequential images, corresponding to a ~90 ms recording time, were collected from one experiment. The level of neuronal activities was indicated with pseudocolor (256 colors). To analyze the time course of activities in a given sample area, data from each pixel were stored, retrieved, and plotted as a function of time using Origin 5.0 (OriginLab, Northampton, MA).

In vitro *kinase assay.* Immunoprecipitates from the hippocampus were suspended in Src kinase reaction buffer (in mM: 100 Tris-HCl, pH 7.5, 125 $MgCl_2$, 25 $MnCl_2$, 2 EGTA, 0.2 sodium orthovanadate, and 2 dithiothreitol). The kinase assay was performed using a Src kinase kit (catalog #17-131; Upstate Biotechnology).

Pharmacological treatment of tissue slices. The hippocampi were quickly dissected and sliced in two directions at a thickness of 350 μm using a McIlwain tissue chopper (Mickle Laboratory Engineering, Gomshall, UK). The hippocampal slices were incubated at 37°C for 1 h in the netwell chamber (Corning, Corning, NY) filled with ACSF, which was continuously saturated with a mixture of 95% O_2/5% CO_2, and then exposed to ACSF in the presence of glutamate (100 μM), glycine (10 μM), and spermidine (1 mM) for 5 min. After a wash in ice-cold ACSF, the slices were homogenized in the modified lysis buffer.

Statistical analysis. All of the data were expressed as mean ± SEM. Statistical differences between the mutant mice and the wild-type mice were determined with Student's *t* comparison test. In the analysis of the visible or hidden test in the Morris water maze test, statistical differences were determined by an ANOVA with repeated measures. In the analysis of the transfer test in the Morris water maze, fear conditioning, and novel object recognition tasks, statistical differences among values for individual groups were determined by ANOVA, followed by the Student–Newman–Keuls multiple comparisons test when *F* ratios were significant ($p < 0.05$).

Results

ShcC/N-Shc, a major phosphotyrosine adapter protein in the mature hippocampus

The gene expression of Shc-related phosphotyrosine adapter proteins was under dynamic regulation during the mammalian brain development (Fig. 1*A*,*B*). The expression level of ShcA, both the mRNA and protein, decreased during perinatal development and almost disappeared by 10 weeks of age. In contrast, that of ShcC increased gradually during postnatal development, with a peak at approximately postnatal day 7 (P7) to P14. However, ShcB mRNA levels remained low and invariable at all of the developmental stages, whereas its protein levels existed relatively high at P7 and P14. *In situ* hybridization analysis of young adults at 10

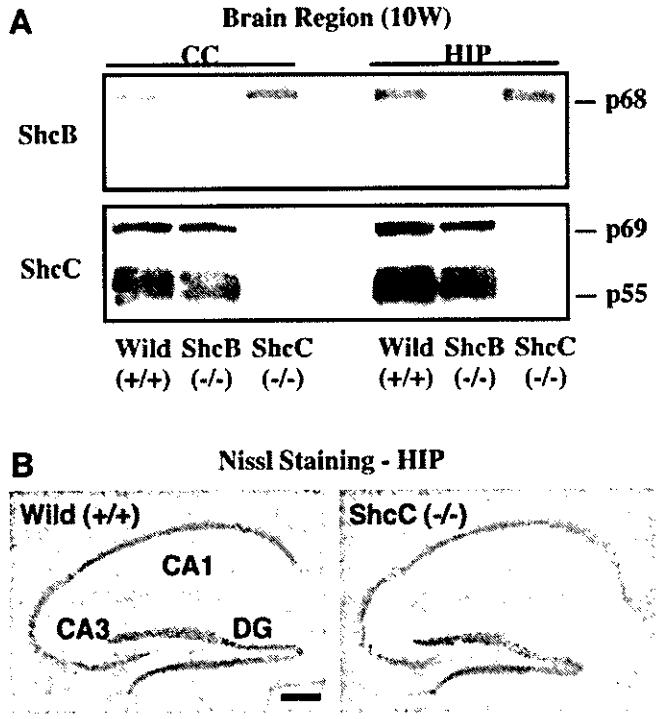

Figure 2. Hippocampal morphology in ShcC mutant mice. *A*, Protein expression of ShcB and ShcC in ShcC mutant mice [10 weeks of age (10W)]. Protein extracts from the cerebral cortex (CC) and hippocampus (HIP) of ShcB and ShcC mutant mice were examined by Western blot analysis. *B*, Nissl staining in the hippocampus of ShcC mutant mice (10W). DG, Dentate gyrus. Scale bar, 200 μm.

weeks of age revealed that ShcC mRNA was highly expressed in the cerebral cortex, hippocampus, and thalamus (Fig. 1*C*). In contrast, the expression of ShcB mRNA was rather ubiquitous (Fig. 1*C*). The regional expression of ShcC protein correlated with the mRNA data, whereas that of ShcB protein was different from mRNA and showed some deviations (i.e., a few high expressions in the hippocampus, thalamus, and midbrain) (Fig. 1*D*). The expression of ShcA was negligible in the various regions of the brain at 10 weeks of age (data not shown). These findings indicate that ShcC is the primary phosphotyrosine adapter protein among the Shc family members in the hippocampus of adult animals.

Histological appearance of hippocampal neurons in ShcC mutant mice

ShcC mutant mice exhibited a complete loss of ShcC protein, but the expression of ShcB was unaffected in most regions of the brain at 10 weeks of age (Fig. 2*A*, cerebral cortex and hippocampus). Neuroanatomically, the hippocampus of ShcC mutant mice revealed no gross structural abnormalities on Nissl staining compared with that of wild-type mice (Fig. 2*B*). MAP2 immunostaining for the dendrites of neurons in the hippocampal CA1 area of the mutant mice gave a pattern indistinguishable from that in wild-type mice (data not shown). Thus, the deficiency of ShcC did not significantly alter the hippocampal morphology in the mature brain.

Enhancement of hippocampus-dependent learning and memory in ShcC mutant mice

To investigate whether a deficiency of ShcC affects neuronal functions of the mature brain, we examined the performance of ShcC mutant mice in several behavioral paradigms. We first tested motor coordination and nociceptive response. The motility in a novel environment was measured for both horizontal (locomotion) and vertical (rearing) activities. Neither locomotion nor rearing during a 60 min observation period differed significantly between the wild-type mice (locomotion, 13,122.2 ± 1197.8 counts; rearing, 70.7 ± 13.8 counts) and ShcC mutant mice (locomotion, 13,355.0 ± 1405.0 counts; rearing, 81.8 ± 14.1 counts). Furthermore, no aberrant nociceptive responses to electric footshocks were observed in the ShcC mutant mice: the footshock threshold in the mutant mice (flinching, 0.045 ± 0.002 mA; vocalizing, 0.233 ± 0.027 mA; jumping, 0.425 ± 0.031 mA) was the same as that in wild-type mice (flinching, 0.045 ± 0.004 mA; vocalizing, 0.228 ± 0.015 mA; jumping, 0.400 ± 0.046 mA). These results indicate no apparent abnormalities in either motor or sensory neuronal systems in the ShcC mutant mice, consistent with previous observations (Sakai et al., 2000).

We next tested spatial and nonspatial learning and memory in ShcC mutant mice using the paradigms of the Morris water maze, fear conditioning, and novel object recognition tasks. In the Morris water maze task, both the wild-type and ShcC mutant mice managed to learn the visible-platform test, but the escape latency to the platform was shorter for the mutant mice (ANOVA with repeated measures; $F_{(1,22)} = 4.446$; $p = 0.0010$) (Fig. 3*Aa*). In the hidden-platform test, which requires the activation of the NMDA receptors in the hippocampus (Morris et al., 1982; Tsien et al., 1996), ShcC mutant mice required less time to reach the platform than wild-type mice (ANOVA with repeated measures; $F_{(1,34)} = 3.689$; $p = 0.0034$) (Fig. 3*Ab*). Swimming speeds of the wild-type and ShcC mutant mice in the visible- and hidden-platform tests were essentially the same (swimming speed on the first day of the hidden-platform test; wild-type mice, 17.9 ± 1.2 cm/s; ShcC mutant mice, 18.6 ± 1.1 cm/s). Moreover, in the platform transfer test conducted after the hidden-platform test, the ShcC mutant mice exhibited greater preference for the trained quadrant than the wild-type mice (Fig. 3*Ac*).

We tested for associative memory in the contextual and cued fear conditioning tasks. The former is hippocampus dependent, whereas the latter is hippocampus independent (Phillips and LeDoux, 1992). Both types of fear conditioning task also require the activation of the NMDA receptors (Davis et al., 1987; Kim et al., 1992). The contextual and cued fear conditioning tasks were measured 24 h after an aversive event (footshock) using two separate sets of genotype groups. The freezing response before the footshock (preconditioning) did not differ between the wild-type and ShcC mutant mice (Fig. 3*B*). In the contextual fear conditioning test, the freezing response 24 h after the footshock in both the wild-type and ShcC mutant mice significantly increased compared with the preconditioning and pseudoconditioning groups, respectively, with the mutant mice exhibiting a much stronger response than wild-type mice (Fig. 3*B*). In contrast, in the cued fear conditioning test, there was no significant difference in the freezing response 24 h after the footshock between the wild-type mice (62.6 ± 5.1%) and ShcC mutant mice (64.6 ± 3.3%).

To examine visual recognition memory in ShcC mutant mice, we used a novel object recognition task, in which the activation of the NMDA receptors in the hippocampus is essential for the formation of recognition memory (Rampon et al., 2000). We used a 5 min training protocol to assess the enhancement of learning and memory. There was no difference in exploratory preference during the training between the wild-type and ShcC mutant mice (Fig. 3*C*), indicating that the two groups essentially had the same levels of curiosity and/or motivation to explore the two objects.

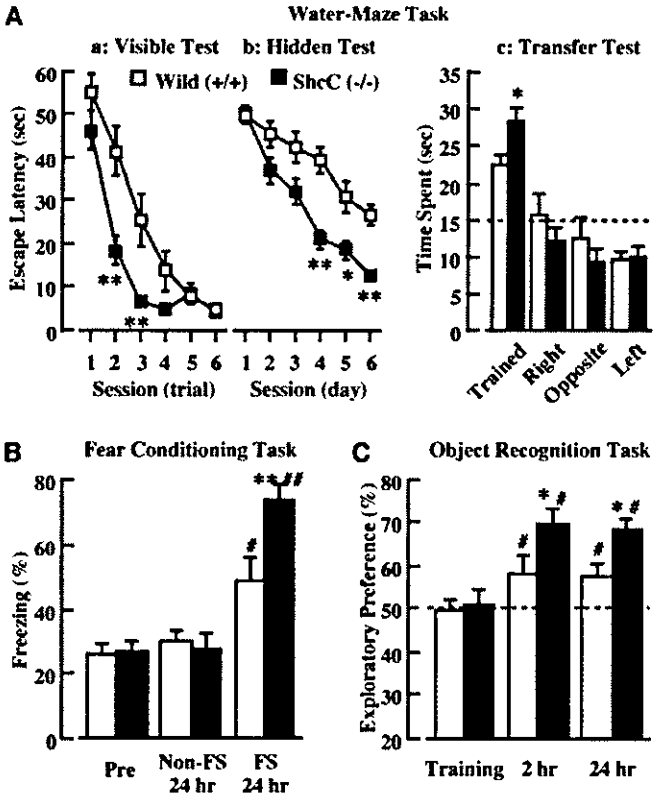

Figure 3. Hippocampus-dependent learning and memory in ShcC mutant mice. ***A***, Morris water maze task. Escape latency in the visible (*a*)- and hidden (*b*)-platform tests. ***c***, The time spent in each quadrant in the transfer test 24 h after the hidden-platform test. The time spent in the trained quadrant was significantly longer than that in any other quadrants in both the wild-type and ShcC mutant mice ($p < 0.05$; Student–Newman–Keuls multiple comparisons test). The dotted line represents performance by chance (15 s). ***B***, Contextual fear conditioning test. The freezing response was measured for 2 min 24 h after the conditioning [FS (footshock)] or pseudoconditioning (Non-FS). ***C***, Novel object recognition test. The time spent exploring two objects was measured for 5 min during training and retention 2 or 24 h after the training. The dotted line represents performance by chance (50%). Data represent mean ± SEM (n = 8–18). $^{*}p < 0.05$ and $^{**}p < 0.01$ versus corresponding wild type (+/+). $^{\#}p < 0.05$ and $^{\#\#}p < 0.01$ versus corresponding non-FS or training value in wild type (+/+).

In 2 and 24 h retention, however, ShcC mutant mice exhibited greater preference toward the novel object than wild-type mice (Fig. 3*C*).

Overall, these findings in the three different paradigms suggest that hippocampus-dependent spatial and nonspatial learning and memory is enhanced in the ShcC mutant mice, and this enhancement reflects neither increased motor activity nor altered nociceptive sensitivity.

Enhancement of hippocampal LTP in ShcC mutant mice

To investigate the synaptic properties in the hippocampus of ShcC mutant mice, we performed electrophysiological analyses using hippocampal slices. We used a high-speed optical recording technique in the hippocampal CA1 area by stimulating Schaffer collateral afferents from the CA3 area. With this technique, the optical signals evoked in the stratum radiatum of the CA1 area were broken down into two distinct elements, an initial spike-like component and an immediately following slow component, which could be separated by a notch in the control (Fig. 4*Aa*, arrow). These components represent the presynaptic fiber volley (PSFV) and EPSP, respectively, because the spike-like component left in Ca^{2+}-free medium (Fig. 4*Ab*) is eliminated by tetrodotoxin (TTX; 1 μM) (Fig. 4*Ad*) and the slow component is

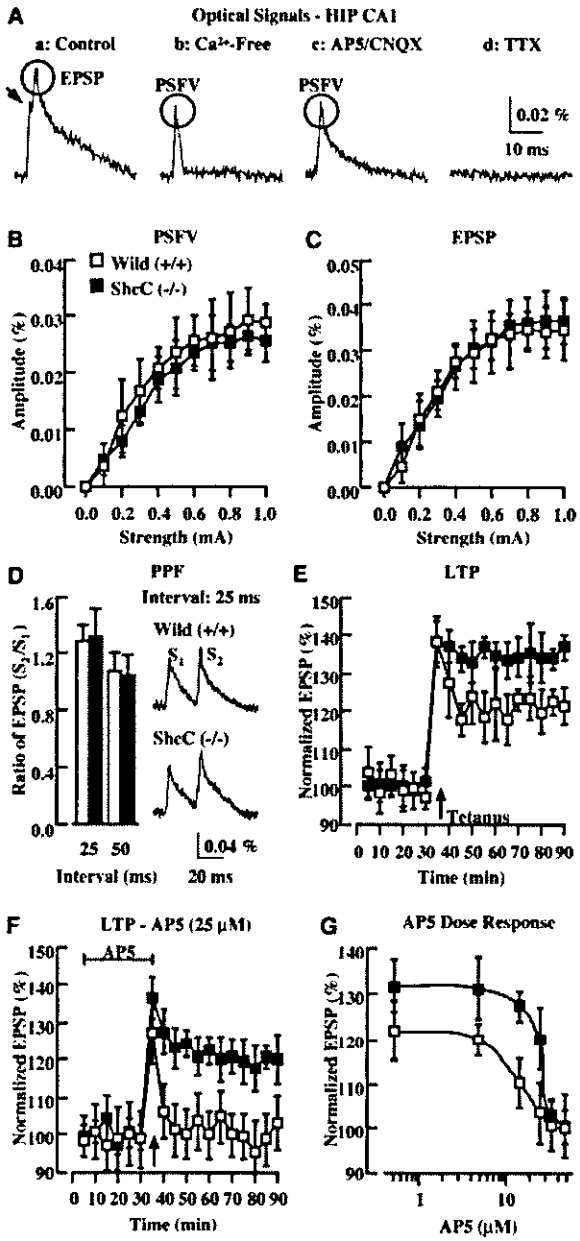

Figure 4. Hippocampal synaptic transmission and LTP in ShcC mutant mice. ***A***, Optical signals in the stratum radiatum of the hippocampal (HIP) CA1 area. Representative traces of optical signal in response to an electrical stimulus of the Schaffer collateral fibers are shown. The control signal (*a*) is composed of PSFV (arrow) and EPSP: the former could be separated by treatment with Ca^{2+}-free medium (*b*) or AP-5 (50 μM)/CNQX (10 μM) (*c*) and eliminated by treatment with TTX (1 μM) (*d*). ***B***, Amplitude of PSFV versus stimulus intensity. ***C***, Amplitude of EPSP versus stimulus intensity. The input–output relationship of PSFV or EPSP is plotted against stimulus intensity at the Schaffer collateral-CA1 synapses (5 slices from 4 wild-type mice; 5 slices from 5 ShcC mutant mice). ***D***, Paired-pulse facilitation (PPF). The data represent the facilitation of the second EPSP (S_2) relative to the first EPSP (S_1). Traces are the synaptic responses evoked by paired-pulse stimulation (interval, 25 ms) (4 slices from 3 wild-type mice; 4 slices from 3 ShcC mutant mice). ***E***, Hippocampal LTP. Each point represents the mean ± SEM EPSP normalized to the baseline EPSP, which was the mean of EPSP for 20–30 min (7 slices from 4 wild-type mice; 7 slices from 4 ShcC mutant mice). Tetanic stimulation induced LTP at 90 min in the wild-type mice (121.2 ± 5.0%) and ShcC mutant mice (136.8 ± 3.4%; $p < 0.05$). ***F***, Treatment with NMDA receptor antagonist AP-5. Each point represents the normalized mean of EPSP ± SEM in the presence of AP-5 (25 μM) for 5–35 min (4 slices from 4 wild-type mice; 6 slices from 4 ShcC mutant mice). Tetanic stimulation with AP-5 treatment failed to induce LTP in the wild-type mice (103.5 ± 7.0% at 90 min), and induced LTP in ShcC mutant mice (120.1 ± 6.7% at 90 min; $p < 0.05$). ***G***, Dose–effect of AP-5 on LTP expression. Each point represents the normalized mean ± SEM EPSP at 60 min after the tetanic stimulation in the presence of different concentrations of AP-5 (4 slices from 4 wild-type mice; 6 slices from 4 ShcC mutant mice) (EC_{50}: wild-type mice, 15.2 μM; ShcC mutant mice, 26.6 μM).

blocked by D-2-amino-5-phosphonovaleric acid (AP-5; 50 μM)/6-cyano-7-nitroquinoxaline-2,3-dione (CNQX; 10 μM), competitive NMDA and AMPA receptor antagonists (Fig. 4*Ac*).

Initial experiments were designed to examine the input–output relationship of synaptic transmission by measuring two distinct components for a range of stimulus intensities. The amplitude of PSFV in the wild-type and ShcC mutant mice was almost the same (Fig. 4*B*), indicating that presynaptic properties were not altered in the mutant mice. There was no difference in the amplitude of EPSP between the wild-type and ShcC mutant mice (Fig. 4*C*), indicating that basal synaptic transmission remains normal in the mutant mice. Similarly, paired-pulse facilitation, which is a short-term enhancement of synaptic efficacy in response to a closely spaced second stimulus and reflects the probability of neurotransmitter release from afferent neurons, differed little between the wild-type and ShcC mutant mice (Fig. 4*D*). These results suggest that synaptic transmission does not deteriorate at the hippocampal Schaffer collateral-CA1 synapses in the ShcC mutant mice.

The LTP in the hippocampal CA1 area, a typical form of synaptic plasticity, is known to involve the activation of the NMDA receptors in its induction. We next examined the synaptic plasticity at hippocampal CA1 synapses using a high-frequency conditioning, tetanic stimulation (100 Hz; 1 s) to induce LTP. There was a marked difference in the expression of hippocampal LTP between the wild-type and ShcC mutant mice (Fig. 4*E*). The early phase of LTP in ShcC mutant mice was consistently enhanced during observation up to 60 min after the tetanic stimulation (wild-type mice, 121.2 ± 5.0%; ShcC mutant mice, 136.8 ± 3.4%; $p < 0.05$) (Fig. 4*E*, EPSP at 90 min). The treatment with AP-5 (25 μM) before the tetanic stimulation in wild-type mice completely blocked the expression of LTP, whereas that in ShcC mutant mice induced LTP (EPSP at 90 min) (wild-type mice, 103.5 ± 7.0%; ShcC mutant mice, 120.1 ± 6.7%; $p < 0.05$) (Fig. 4*F*). As shown in Figure 4*G*, AP-5 dose-dependently inhibited the expression of LTP in both the wild-type and ShcC mutant mice, but with different EC_{50} values of AP-5 between the two groups (wild-type mice, 15.2 μM; ShcC mutant mice, 26.6 μM). These results suggest that the enhancement of hippocampal LTP in ShcC mutant mice would arise from the functional alteration of postsynaptic NMDA receptors in the hippocampal CA1 area, because presynaptic function is normal in this area.

Increased phosphorylation of the NMDA receptors in the hippocampus of ShcC mutant mice

The NMDA receptors are formed by NR1 (GluRζ1) and NR2A to NR2D (GluRε1 to GluRε4) subunits (Hollmann and Heinemann, 1994; Nakanishi and Masu, 1994), and their activity is modulated by either the subunit composition of the receptor (Kutsuwada et al., 1992; Monyer et al., 1994) or phosphorylation of the subunits (Wang and Salter, 1994; Yu et al., 1997). To investigate NMDA receptor activity in the hippocampus of ShcC mutant mice, we examined the expression and phosphorylation levels of the receptor subunits. There was no difference in the expression level of the NR2A, NR2B, or NR1 subunit in the hippocampus between the wild-type and ShcC mutant mice (Fig. 5*A*). The expression level of PSD95, which regulates the signaling by the NMDA receptors, was the same in ShcC mutant mice as in wild-type mice (Fig. 5*A*). However, the tyrosine phosphorylation level of NR2A or NR2B in ShcC mutant mice showed a significant increase compared with that in wild-type mice (Fig. 5*A*). These findings suggest that the basal function of the NMDA receptors in the hippocampus of ShcC mutant mice is enhanced by the hyperphosphorylation at tyrosine residues of the receptor subunits.

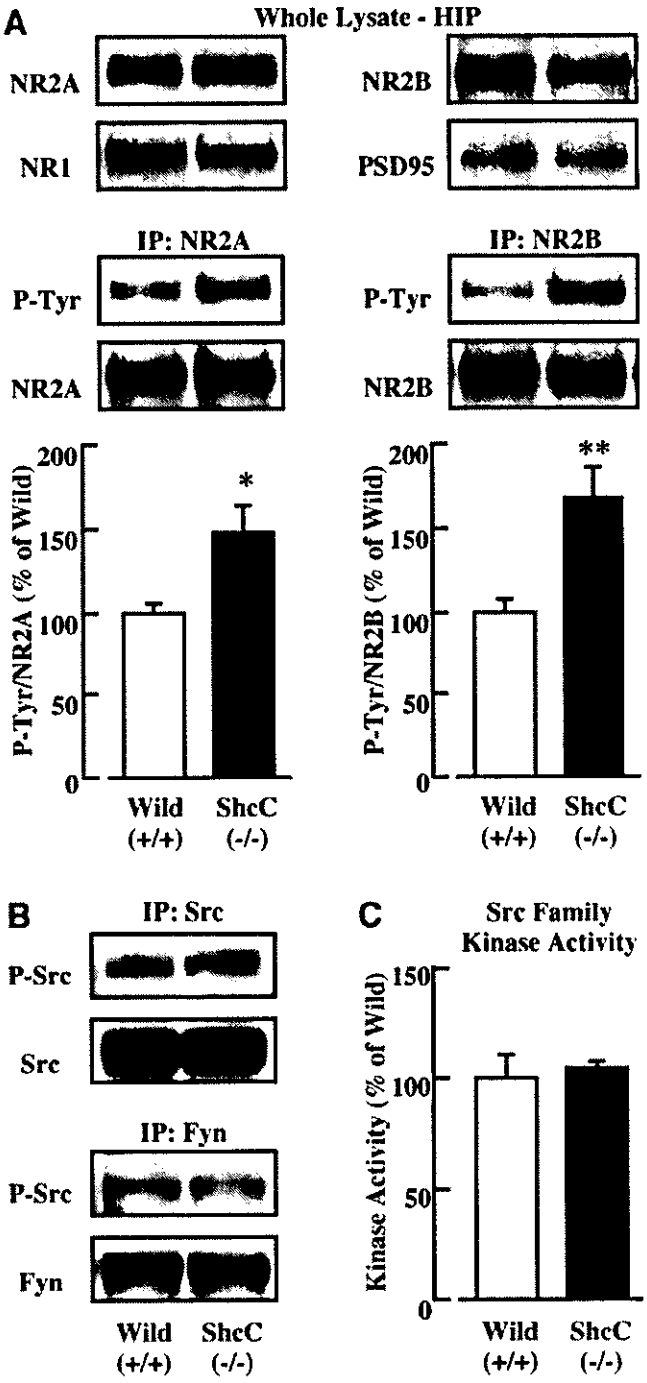

Figure 5. Phosphorylation of the NMDA receptors and kinase activity of the Src family in the hippocampus of ShcC mutant mice. ***A***, Expression and tyrosine phosphorylation of the NR2A and NR2B subunits. The whole lysates of the hippocampus (HIP) were immunoblotted with anti-NR2A, -NR2B, -NR1, or -PSD95 antibody. To dissociate the NMDA receptor complex, hippocampal lysates with a modified lysis buffer were boiled for 5 min. The immunoprecipitates (IP) obtained with anti-NR2A or -NR2B antibody were immunoblotted with anti-phosphotyrosine (P-Tyr) antibody. ***B***, Tyrosine phosphorylation at the activation site of Src and Fyn. The immunoprecipitates prepared with anti-Src or -Fyn antibody were immunoblotted with anti-phospho-Src (P-Src) family antibody. ***C***, Kinase activity of the Src family *in vitro*. The immunoprecipitates obtained with anti-Src family antibody were subjected to an *in vitro* Src kinase assay. Data represent mean ± SEM ($n = 4$). $^{*}p < 0.05$ and $^{**}p < 0.01$ versus corresponding wild type (+/+).

Because the tyrosine phosphorylation of subunits NR2A and NR2B of the NMDA receptors is known to be modulated by the

Src family of cytoplasmic tyrosine kinases, including Src and Fyn (Hisatsune et al., 1999; Nakazawa et al., 2001), we tested the kinase activity of this family in the hippocampus of ShcC mutant mice. However, there was no notable difference in the tyrosine phosphorylation level at the activation site of Src or Fyn between the wild-type and ShcC mutant mice (Fig. 5*B*). Moreover, the kinase activity of the Src family in the mutant mice was similar to that in wild-type mice (Fig. 5*C*). These results indicate that increased tyrosine phosphorylation of the NMDA receptors in the ShcC mutant mice is not attributable to the activation of Src and Fyn.

Interaction of ShcC/N-Shc with the NMDA receptors and the Src family in the hippocampus

To clarify the regulatory mechanism of ShcC in NMDA receptor function involved in hippocampal synaptic plasticity, we investigated whether ShcC interacts with the NMDA receptors and the Src family. In an immunoprecipitation assay using lysates prepared from the hippocampus of wild-type mice, the NR1 or NR2B subunit of the NMDA receptors coprecipitated greatly with ShcC compared with other Shc family members (Fig. 6*A*). Similarly, Src (or Fyn) also interacted with ShcC (Fig. 6*A*). To further test whether these interactions would be affected by the activation of excitatory synaptic transmission, we examined the interaction between ShcC and the NR2B subunit or the Src family under conditions of glutamate stimulation in hippocampal slices from wild-type mice. After a 5 min stimulation with glutamate (100 μM) in the presence of glycine (10 μM) and spermidine (1 mM), both endogenous coactivators for the NMDA receptors, the amount of NR2B subunit coimmunoprecipitated with ShcC increased significantly (Fig. 6*B*). In the same conditions, the interaction of Src (or Fyn) with ShcC also increased significantly (Fig. 6*B*). These findings indicate that ShcC binds to the NMDA receptors and also associates with Src and/or Fyn in the mature hippocampus, and the formation of this ternary complex is stimulated by the activation of the excitatory glutamatergic neuronal system.

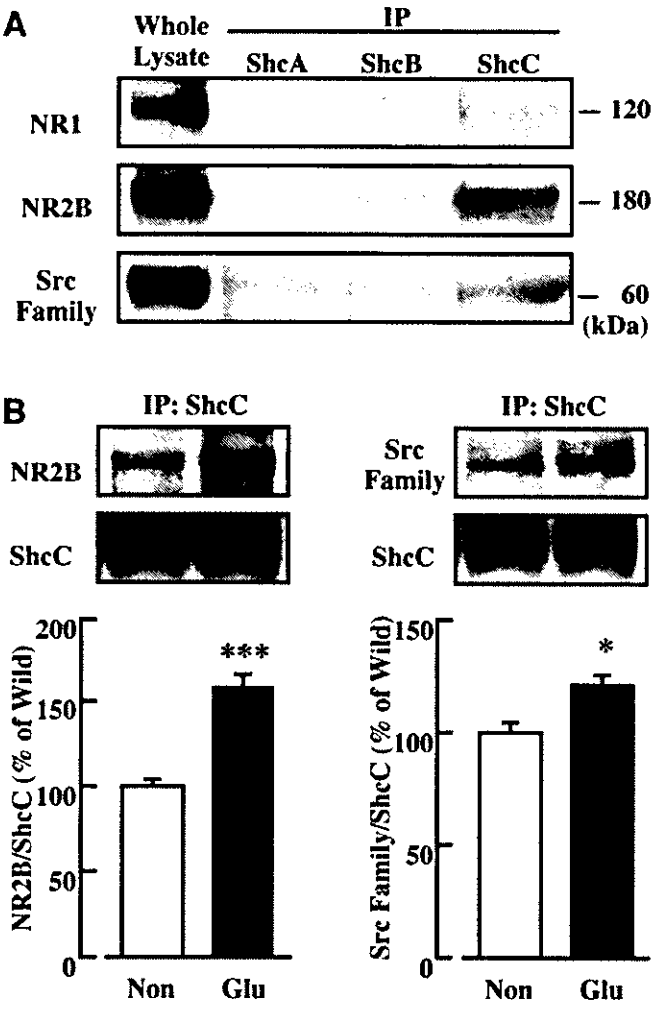

Figure 6. Interaction of ShcC with the NMDA receptors and the Src family in the hippocampus. ***A***, Coimmunoprecipitation with Shc family members in the hippocampus. The immunoprecipitates (IP) obtained with antibodies for ShcA, ShcB, or ShcC were immunoblotted with anti-NR1, -NR2B, or -Src family antibody. ***B***, Coimmunoprecipitation with ShcC in the hippocampus after glutamate (Glu) stimulation. Hippocampal slices were treated with glutamate (100 μM)/glycine (10 μM)/spermidine (1 mM) for 5 min. The immunoprecipitates (IP) prepared with anti-ShcC antibody were immunoblotted with anti-NR2B or -Src family antibody. Data represent mean ± SEM ($n = 4$). *$p < 0.05$ and ***$p < 0.001$ versus corresponding wild type (+/+).

Discussion

In the present study, we demonstrated that the phosphotyrosine adapter protein ShcC/N-Shc is implicated in the modulation of hippocampal synaptic plasticity. However, as described in Introduction, hippocampal LTP may not rely on the Shc-mediated TrkB-Ras/MAPK signaling (Korte et al., 2000; Minichiello et al., 2002). Rather than the Shc/Ras/MAPK pathway, the PLCγ/IP3/CaMKIV pathway may be more relevant to the modulation of hippocampal LTP immediately downstream of the TrkB receptor (Minichiello et al., 2002). Thus, our results were unexpected, and we were interested in the novel role of ShcC to modulate the hippocampal LTP underlying learning and memory. We therefore estimate that the role of ShcC in hippocampal synaptic plasticity is independent of the Ras/MAPK pathway from the TrkB receptor and is critical to the modulation of NMDA receptor function, based on the attenuated effect of an NMDA receptor antagonist on LTP expression and the increased tyrosine phosphorylation of the NMDA receptors in the hippocampus of ShcC mutant mice.

Role of ShcC/N-Shc in hippocampal synaptic plasticity via interaction with the NMDA receptor

We have shown here that ShcC specifically interacted with the NR2B subunit of the NMDA receptors and Src (or Fyn) of tyrosine kinases in the hippocampus, and these interactions were enhanced by glutamate stimulation. The NR2B subunit is phosphorylated at several tyrosine residues by Src and Fyn (Hisatsune et al., 1999; Nakazawa et al., 2001), and the phosphorylation levels are upregulated by tetanic stimulation to induce hippocampal LTP (Rosenblum et al., 1996; Rostas et al., 1996). Thus, it is plausible that ShcC affects NMDA receptor function by binding to the receptor subunit via its phosphotyrosine binding property in an activity-dependent manner. Therefore, ShcC would regulate the receptor activation in the hippocampal LTP through Src family kinase-mediated tyrosine phosphorylation.

The elevated tyrosine phosphorylation levels of NMDA receptor subunits and normal kinase activity levels of the Src family in the hippocampus of ShcC mutant mice suggest that ShcC is implicated in the dephosphorylation of the receptor subunits. If the phosphorylation of the NMDA receptors is downregulated in the presence of ShcC, a potential role of ShcC could be to recruit a certain protein tyrosine phosphatase to the receptor multicomplex or to activate directly or indirectly a phosphatase for phosphotyrosine residues on the receptor subunits. Thus, ShcC binds

the phosphorylated NMDA receptor subunits and also may modulate the dephosphorylation status of the receptor subunits. Alternatively, if the NMDA receptor phosphorylation is upregulated in the presence of ShcC, the interaction of ShcC with a phosphorylated tyrosine of the receptor subunits may mask other tyrosine residues on the subunits from additional phosphorylation by the Src family. Otherwise, ShcC may inhibit activation of an unknown tyrosine kinase for the receptor subunits. Therefore, ShcC would contribute to the interaction between Src-like tyrosine kinase and a tyrosine phosphatase around the NMDA receptor multicomplex, to modulate the hippocampal synaptic plasticity via the receptor activation.

In general, synaptic plasticity is considered a leading candidate for a cellular mechanism of learning and memory (Bliss and Collingridge, 1993; Malenka and Nicoll, 1999), and a good correlation between NMDA receptor-dependent LTP and spatial learning and memory has been demonstrated (Tsien et al., 1996; Tang et al., 1999). Therefore, the superior hippocampus-dependent learning and memory in ShcC mutant mice would be primarily caused by the enhanced NMDA receptor-dependent hippocampal LTP. As evidence to support the above estimation, the difference in the performance of ShcC mutant mice between the contextual and cued fear conditioning tasks should be mentioned. The contextual associative memory is hippocampus dependent, whereas the cued associative memory is hippocampus independent (Phillips and LeDoux, 1992). Both associative memories also depend on the amygdala (Lavond et al., 1993) and NMDA receptor activation (Davis et al., 1987; Kim et al., 1992). Thus, the enhancement of only the former in ShcC mutant mice suggests the specific activation of the NMDA receptors in the hippocampus of the mutant mice.

However, the enhancement of behavioral performance in ShcC mutant mice was observed not only in the hidden-platform test of the Morris water maze task that depends on the hippocampus but also in the visible-platform test that is not necessarily hippocampus dependent. Thus, the performance of ShcC mutant mice in the present behavioral tasks may not be affected by only a specific improvement of hippocampus-dependent learning and memory. There are several explanations for the better performance of ShcC mutant mice in the latter test (e.g., the alteration of motility, emotionality, and visual acuity). Although there was at least no difference in the motility, especially swimming ability, of ShcC mutant mice, emotionality such as motivation to escape from water may be affected by alterations of NMDA receptor function in the hippocampus, because the alterations are known to influence emotion-associated neuronal circuits in other regions of the brain (e.g., the dopaminergic and serotonergic neuronal systems in the cerebral cortex and striatum) (Mohn et al., 1999; Miyamoto et al., 2001). Currently, there is no evidence that ShcC is involved in emotionality and those neuronal systems. However, because ShcC is expressed in the retinal ganglion cell during perinatal development (Nakazawa et al., 2002), a loss of ShcC may have some influence on the performance of visual acuity. Therefore, there is a need to investigate the emotional and visual performance in ShcC mutant mice.

Upstream and downstream signaling of the ShcC/N-Shc associated with hippocampal synaptic plasticity

We discussed above that ShcC plays a role in the modulation of hippocampal synaptic plasticity via interaction with the postsynaptic NMDA receptors but not with the BDNF-stimulated TrkB receptors. This idea is consistent with the findings that ShcC accumulates in the PSD (Suzuki et al., 1999) and BDNF is required for presynaptic but not postsynaptic modulation of LTP in the hippocampal CA3–CA1 synapses (Xu et al., 2000; Zakharenko et al., 2003). However, it remains possible that ShcC is involved in TrkB-mediated hippocampal synaptic plasticity at the postsynapses, because BDNF was taken up by postsynaptic neurons in an activity-dependent manner (Kohara et al., 2001). Thus, the enhanced hippocampal LTP in ShcC mutant mice may be caused in part by alterations of postsynaptic TrkB receptor signaling, for example, through activation of the PLCγ-mediated TrkB–IP3/CaMKIV pathway that is proposed to be relevant to hippocampal LTP (Minichiello et al., 2002). More studies are needed to clarify the signaling capabilities of the BDNF-stimulated TrkB receptors in the absence of ShcC and the signaling ability of ShcC as a go-between adapter protein for the TrkB and NMDA receptors, because NMDA receptor activation is frequently associated with TrkB-mediated hippocampal LTP (Suen et al., 1997; Levine et al., 1998). In addition, it is essential to investigate directly the NMDA receptor synaptic responses in ShcC mutant mice, because our findings showed only differences in the contribution of NMDA receptor to hippocampal LTP in the mutant mice.

Similarly to ShcC mutant mice, mice lacking H-Ras showed enhanced hippocampal LTP and tyrosine phosphorylation of the NMDA receptors (Manabe et al., 2000). These enhancements explained why the deficiency of H-Ras increased Src kinase activity and subsequently potentiated the receptor function associated with hippocampal LTP (Thornton et al., 2003). These findings might suggest that ShcC modulates NMDA receptor function for hippocampal LTP via inhibition of Src kinase activity through the Ras family, including H-Ras, because ShcC transmits BDNF-stimulated TrkB receptor signaling to the Ras/MAPK pathway (Nakamura et al., 1998; Liu and Meakin, 2002). In this study, however, Src and Fyn kinase activity were unaffected in the hippocampus of ShcC mutant mice, which was distinct from the case of H-Ras mutant mice.

Hippocampal synaptic modulation by ShcC may also involve other molecules. A novel 250 kDa Rho-GTPase activating protein (GAP) Grit (Nakamura et al., 2002), also termed RICS (Rho GAP involved in the β-catenin–N-cadherin and NMDA receptor signaling) (Okabe et al., 2003) or p250GAP (Nakazawa et al., 2003), is suggested to be involved in modulation of NMDA receptor signaling. Grit was identified originally as a binding partner of ShcC and is involved in neurotrophin-dependent neurite outgrowth via the specific modulation of cytoskeletal actin dynamics (Nakamura et al., 2002). Actin dynamics in dendritic spines have been implicated in hippocampal LTP (Engert and Bonhoeffer, 1999; Matus, 2000). Grit interacted with the NR2B subunit of the NMDA receptors, and this interaction was modulated by the receptor activation (Nakazawa et al., 2003). These findings suggest that Grit regulates the NMDA receptor-dependent actin reorganization in dendritic spines. Thus, the absence of ShcC may also influence the localization of Grit and further affect the postsynaptic remodeling of the cytoskeleton underneath the NMDA receptors, which is associated with hippocampal LTP underlying learning and memory (Milner et al., 1998). It could be that multiple molecules are needed to regulate synaptic function for hippocampal LTP (Sanes and Lichtman, 1999; Inoue and Okabe, 2003); however, ShcC would be a modulatory component of these molecules at the hippocampal synapses.

In summary, our observations revealed that the enhancement of hippocampal LTP in ShcC mutant mice is primarily attributable to an alteration of NMDA receptor function rather than an effect on the TrkB–Shc site. The current study established that the

neural-specific phosphotyrosine adapter protein ShcC/N-Shc is a modulator of hippocampal synaptic plasticity underlying learning and memory.

References

Adams JP, Sweatt JD (2002) Molecular psychology: roles for the ERK MAP kinase cascade in memory. Annu Rev Pharmacol Toxicol 42:135–163.

Bliss TV, Collingridge GL (1993) A synaptic model of memory: long-term potentiation in the hippocampus. Nature 361:31–39.

Cattaneo E, Pelicci PG (1998) Emerging roles for SH2/PTB-containing Shc adaptor proteins in the developing mammalian brain. Trends Neurosci 21:476–481.

Davis M, Hitchcock J, Rosen JB (1987) Anxiety and the amygdala: pharmacological and anatomical analysis of the fear-potentiated startle paradigm. In: The psychology of learning and motivation (Bower GH, ed), pp 263–305. New York: Academic.

Engert F, Bonhoeffer T (1999) Dendritic spine changes associated with hippocampal long-term synaptic plasticity. Nature 399:66–70.

Hisatsune C, Umemori H, Mishina M, Yamamoto T (1999) Phosphorylation-dependent interaction of the *N*-methyl-D-aspartate receptor ε2 subunit with phosphatidylinositol 3-kinase. Genes Cells 4:657–666.

Hollmann M, Heinemann S (1994) Cloned glutamate receptors. Annu Rev Neurosci 17:31–108.

Inoue A, Okabe S (2003) The dynamic organization of postsynaptic proteins: translocating molecules regulate synaptic function. Curr Opin Neurobiol 13:332–340.

Kaplan DR, Miller FD (2000) Neurotrophin signal transduction in the nervous system. Curr Opin Neurobiol 10:381–391.

Kim JJ, Fanselow MS, DeCola JP, Landeira-Fernandez J (1992) Selective impairment of long-term but not short-term conditional fear by the *N*-methyl-D-aspartate antagonist APV. Behav Neurosci 106:591–596.

Kohara K, Kitamura A, Morishima M, Tsumoto T (2001) Activity-dependent transfer of brain-derived neurotrophic factor to postsynaptic neurons. Science 291:2419–2423.

Kojima T, Yoshikawa Y, Takada S, Sato M, Nakamura T, Takahashi N, Copeland NG, Gilbert DJ, Jenkins NA, Mori N (2001) Genomic organization of the Shc-related phosphotyrosine adapters and characterization of the full-length Sck/ShcB: specific association of p68-Sck/ShcB with pp135. Biochem Biophys Res Commun 284:1039–1047.

Korte M, Minichiello L, Klein R, Bonhoeffer T (2000) Shc-binding site in the TrkB receptor is not required for hippocampal long-term potentiation. Neuropharmacology 39:717–724.

Kutsuwada T, Kashiwabuchi N, Mori H, Sakimura K, Kushiya E, Araki K, Meguro H, Masaki H, Kumanishi T, Arakawa M, Mishina M (1992) Molecular diversity of the NMDA receptor channel. Nature 358:36–41.

Lavond DG, Kim JJ, Thompson RF (1993) Mammalian brain substrates of aversive classical conditioning. Annu Rev Psychol 44:317–342.

Levine ES, Crozier RA, Black IB, Plummer MR (1998) Brain-derived neurotrophic factor modulates hippocampal synaptic transmission by increasing *N*-methyl-D-aspartic acid receptor activity. Proc Natl Acad Sci USA 95:10235–10239.

Liu HY, Meakin SO (2002) ShcB and ShcC activation by the Trk family of receptor tyrosine kinases. J Biol Chem 277:26046–26056.

Lu B (2003) BDNF and activity-dependent synaptic modulation. Learn Mem 10:86–98.

Malenka RC, Nicoll RA (1999) Long-term potentiation—a decade of progress? Science 285:1870–1874.

Manabe T, Aiba A, Yamada A, Ichise T, Sakagami H, Kondo H, Katsuki M (2000) Regulation of long-term potentiation by H-Ras through NMDA receptor phosphorylation. J Neurosci 20:2504–2511.

Matus A (2000) Actin-based plasticity in dendritic spines. Science 290:754–758.

Milner B, Squire LR, Kandel ER (1998) Cognitive neuroscience and the study of memory. Neuron 20:445–468.

Minichiello L, Calella AM, Medina DL, Bonhoeffer T, Klein R, Korte M (2002) Mechanism of TrkB-mediated hippocampal long-term potentiation. Neuron 36:121–137.

Miyamoto Y, Yamada K, Noda Y, Mori H, Mishina M, Nabeshima T (2001) Hyperfunction of dopaminergic and serotonergic neuronal systems in mice lacking the NMDA receptor epsilon1 subunit. J Neurosci 21:750–757.

Mohn AR, Gainetdinov RR, Caron MG, Koller BH (1999) Mice with reduced NMDA receptor expression display behaviors related to schizophrenia. Cell 98:427–436.

Monyer H, Burnashev N, Laurie DJ, Sakmann B, Seeburg PH (1994) Developmental and regional expression in the rat brain and functional properties of four NMDA receptors. Neuron 12:529–540.

Morris RG, Garrud P, Rawlins JN, O'Keefe J (1982) Place navigation impaired in rats with hippocampal lesions. Nature 24:681–683.

Nakamura T, Muraoka S, Sanokawa R, Mori N (1998) N-Shc and Sck, two neuronally expressed Shc adapter homologs. Their differential regional expression in the brain and roles in neurotrophin and Src signaling. J Biol Chem 273:6960–6967.

Nakamura T, Komiya M, Sone K, Hirose E, Gotoh N, Morii H, Ohta Y, Mori N (2002) Grit, a GTPase-activating protein for the Rho family, regulates neurite extension through association with the TrkA receptor and N-Shc and CrkL/Crk adapter molecules. Mol Cell Biol 22:8721–8734.

Nakanishi S, Masu M (1994) Molecular diversity and functions of glutamate receptors. Annu Rev Biophys Biomol Struct 23:319–348.

Nakazawa T, Komai S, Tezuka T, Hisatsune C, Umemori H, Semba K, Mishina M, Manabe T, Yamamoto T (2001) Characterization of Fyn-mediated tyrosine phosphorylation sites on GluR ε2 (NR2B) subunit of the *N*-methyl-D-aspartate receptor. J Biol Chem 276:693–699.

Nakazawa T, Nakano I, Sato M, Nakamura T, Tamai M, Mori N (2002) Comparative expression profiles of Trk receptors and Shc-related phosphotyrosine adapters during retinal development: potential roles of N-Shc/ShcC in brain-derived neurotrophic factor signal transduction and modulation. J Neurosci Res 68:668–680.

Nakazawa T, Watabe AM, Tezuka T, Yoshida Y, Yokoyama K, Umemori H, Inoue A, Okabe S, Manabe T, Yamamoto T (2003) p250GAP, a novel brain-enriched GTPase-activating protein for Rho family GTPases, is involved in the *N*-methyl-D-aspartate receptor signaling. Mol Biol Cell 14:2921–2934.

Ohno M, Frankland PW, Chen AP, Costa RM, Silva AJ (2001) Inducible, pharmacogenetic approaches to the study of learning and memory. Nat Neurosci 4:1238–1243.

Okabe T, Nakamura T, Nishimura YN, Kohu K, Ohwada S, Morishita Y, Akiyama T (2003) RICS, a novel GTPase-activating protein for Cdc42 and Rac1, is involved in the β-catenin-N-cadherin and *N*-methyl-D-aspartate receptor signaling. J Biol Chem 278:9920–9927.

Patapoutian A, Reichardt LF (2001) Trk receptors: mediators of neurotrophin action. Curr Opin Neurobiol 11:272–280.

Phillips RG, LeDoux JE (1992) Differential contribution of amygdala and hippocampus to cued and contextual fear conditioning. Behav Neurosci 106:274–285.

Poo MM (2001) Neurotrophins as synaptic modulators. Nat Rev Neurosci 2:24–32.

Rampon C, Tang YP, Goodhouse J, Shimizu E, Kyin M, Tsien JZ (2000) Enrichment induces structural changes and recovery from nonspatial memory deficits in CA1 NMDAR1-knockout mice. Nat Neurosci 3:238–244.

Ravichandran KS (2001) Signaling via Shc family adapter proteins. Oncogene 20:6322–6330.

Rosenblum K, Dudai Y, Richter-Levin G (1996) Long-term potentiation increases tyrosine phosphorylation of the *N*-methyl-D-aspartate receptor subunit 2B in rat dentate gyrus *in vivo*. Proc Natl Acad Sci USA 93:10457–10460.

Rostas JA, Brent VA, Voss K, Errington ML, Bliss TV, Gurd JW (1996) Enhanced tyrosine phosphorylation of the 2B subunit of the *N*-methyl-D-aspartate receptor in long-term potentiation. Proc Natl Acad Sci USA 93:10452–10456.

Sakai R, Henderson JT, O'Bryan JP, Elia AJ, Saxton TM, Pawson T (2000) The mammalian ShcB and ShcC phosphotyrosine docking proteins function in the maturation of sensory and sympathetic neurons. Neuron 28:819–833.

Sanes JR, Lichtman JW (1999) Can molecules explain long-term potentiation? Nat Neurosci 2:597–604.

Silva AJ (2003) Molecular and cellular cognitive studies of the role of synaptic plasticity in memory. J Neurobiol 54:224–237.

Suen PC, Wu K, Levine ES, Mount HT, Xu JL, Lin SY, Black IB (1997) Brain-derived neurotrophic factor rapidly enhances phosphorylation of the postsynaptic *N*-methyl-D-aspartate receptor subunit 1. Proc Natl Acad Sci USA 94:8191–8195.

Suzuki T, Mitake S, Murata S (1999) Presence of up-stream and down-

stream components of a mitogen-activated protein kinase pathway in the PSD of the rat forebrain. Brain Res 840:36–44.

Tang YP, Shimizu E, Dube GR, Rampon C, Kerchner GA, Zhuo M, Liu G, Tsien JZ (1999) Genetic enhancement of learning and memory in mice. Nature 401:63–69.

Thornton C, Yaka R, Dinh S, Ron D (2003) H-Ras modulates NMDA receptor function via inhibition of Src tyrosine kinase activity. J Biol Chem 278:23823–23829.

Tsien JZ, Huerta PT, Tonegawa S (1996) The essential role of hippocampal CA1 NMDA receptor-dependent synaptic plasticity in spatial memory. Cell 87:1327–1338.

Wang YT, Salter MW (1994) Regulation of NMDA receptors by tyrosine kinases and phosphatases. Nature 369:233–235.

Xu B, Gottschalk W, Chow A, Wilson RI, Schnell E, Zang K, Wang D, Nicoll RA, Lu B, Reichardt LF (2000) The role of brain-derived neurotrophic factor receptors in the mature hippocampus: modulation of long-term potentiation through a presynaptic mechanism involving TrkB. J Neurosci 20:6888–6897.

Ying SW, Futter M, Rosenblum K, Webber MJ, Hunt SP, Bliss TV, Bramham CR (2002) Brain-derived neurotrophic factor induces long-term potentiation in intact adult hippocampus: requirement for ERK activation coupled to CREB and upregulation of Arc synthesis. J Neurosci 22:1532–1540.

Yu XM, Askalan R, Keil II GJ, Salter MW (1997) NMDA channel regulation by channel-associated protein tyrosine kinase Src. Science 275:674–678.

Zakharenko SS, Patterson SL, Dragatsis I, Zeitlin SO, Siegelbaum SA, Kandel ER, Morozov A (2003) Presynaptic BDNF required for a presynaptic but not postsynaptic component of LTP at hippocampal CA1–CA3 synapses. Neuron 39:975–990.

Zamanillo D, Sprengel R, Hvalby O, Jensen V, Burnashev N, Rozov A, Kaiser KM, Koster HJ, Borchardt T, Worley P, Lubke J, Frotscher M, Kelly PH, Sommer B, Andersen P, Seeburg PH, Sakmann B (1999) Importance of AMPA receptors for hippocampal synaptic plasticity but not for spatial learning. Science 284:1805–1811.

Oncogene (2005) 00, 1–10

www.nature.com/onc

ORIGINAL PAPER

Domain-specific function of ShcC docking protein in neuroblastoma cells

Izumi Miyake[1,2], Yuko Hakomori[1], Yoko Misu[2], Hisaya Nakadate[2], Nobuo Matsuura[2], Michiie Sakamoto[3] and Ryuichi Sakai*[,1]

[1]*Growth Factor Division, National Cancer Center Research Institute, 5-1-1 Tsukiji, Chuo-ku, Tokyo 104-0045, Japan;* [2]*Department of Pediatrics, Kitasato University School of Medicine, 1-15-1 Kitasato, Sagamihara-shi, Kanagawa 228-8555, Japan;* [3]*Department of Pathology, Keio University School of Medicine, 35 Shinanomachi, Shinjuku-ku, Tokyo 160-8582, Japan*

ShcC is a family member of the Shc docking proteins that possess two different phosphotyrosine-binding motifs and conduct signals as Grb2-binding substrates of various receptor tyrosine kinases. We have recently shown that some neuroblastoma cell lines, such as NB-39-nu cells, express a protein complex of hyperphosphorylated ShcC and anaplastic lymphoma kinase (ALK), which is self-activated by gene amplification. Here, we demonstrate that the expression of a mutant ShcC lacking Grb2-binding sites, 3YF-ShcC, significantly impaired the survival, differentiation and motility of NB-39-nu cells by blocking the ERK and Akt pathways. On the other hand, cells overexpressing ShcC or 3YF-ShcC, but not a mutant ShcC that lacks SH2, showed decreased anchorage independency and *in vivo* tumorigenicity, suggesting a novel ShcC-specific suppressive effect through its SH2 domain on cell transformation. Notably, overexpression of ShcC suppressed the sustained phosphorylation of Src family kinase after cell detachment, which might be independent of phosphorylation of Grb2-binding site. It was indicated that the Src/Fyn-Cas pathway is modulated as a target of these suppressive effects by ShcC. Reciprocal change of ShcC expression and phosphorylation observed in malignant neuroblastoma cell lines might be explained by these phosphotyrosine-dependent and -independent functions of ShcC.
Oncogene (2005) **0**, 000–000. doi:10.1038/sj.onc.1208523

Keywords: ShcC; neuroblastoma; dominant-negative form; SH2 domain; Src family kinase

Introduction

The Shc family of docking proteins plays an essential role in leading cellular signaling to specific downstream molecules such as the Ras-ERK pathway and the phosphatidylinositol 3-kinase (PI3K)-Akt pathway when recruited towards phosphotyrosine residues of various activated RTKs. In mammals, three *shc* genes have been identified, and their products have been termed ShcA/Shc, ShcB/Sli/Sck and ShcC/Rai/N-Shc (Nakamura *et al.*, 1996a; O'Bryan *et al.*, 1996b; Pelicci *et al.*, 1996). ShcA is ubiquitously expressed in most organs except the adult neural system, whereas ShcB and ShcC proteins are selectively expressed in the neural system within adult mouse tissues.

The Shc family molecules have a unique PTB-CH1-SH2 modular organization. Two phosphotyrosine-binding modules, PTB and SH2 domains, recognize phosphotyrosine-containing polypeptides such as cytoplasmic domains of various activated RTKs (Pelicci *et al.*, 1992; van der Geer *et al.*, 1995). The CH1 domain has several tyrosine phosphorylation sites that recruit other SH2-containing adaptor molecules such as Grb2 (van der Geer *et al.*, 1996; Thomas and Bradshaw, 1997) and a proline-rich stretch of ShcA composing the binding site for the SH3 domains of other proteins including Src, Fyn and Lyn (Weng *et al.*, 1994; Wary *et al.*, 1998). There might be difference in the molecular functions of each Shc family member, although there is not much information on individual roles of Shc families in the neural system and neuronal tumors.

We have recently shown that the expression and tyrosine phosphorylation of Shc family proteins, especially ShcC, are observed in most neuroblastoma cells. Stable association of constitutively activated anaplastic lymphoma kinase (ALK) with the ShcC has been observed in several neuroblastoma cell lines that have extremely high phosphorylation levels of ShcC (Miyake *et al.*, 2002). These cell lines showed malignant phenotypes as for tumorigenicity in nude mice or soft agar colony assay, and notably, ShcC expression is low compared with other neuroblastoma in spite of significantly high phosphorylation state. The *ALK* gene locus was significantly amplified in these cell lines, which results in the constitutive activation of the ALK and most prominent tyrosine phosphorylation of ShcC among several known binding partners of ALK such as PLCγ and IRS-1 (Miyake *et al.*, 2002).

ALK protein has the typical structure of an RTK classified into the insulin receptor superfamily. It is dominantly expressed in the normal neural system (Iwahara *et al.*, 1997; Morris *et al.*, 1997), although the biological role of this protein in neuronal cells has not yet been clearly identified. We detected remarkable

*Correspondence: R Sakai; E-mail: rsakai@gan2.res.ncc.go.jp
Received 12 October 2004; revised 30 December 2004; accepted 12 January 2005

amplification of the *ALK* gene in three out of 13 neuroblastoma cell lines (Miyake *et al.*, 2002) and a less significant gain of copy numbers in eight out of 85 primary neuroblastoma tissues (Hakomori *et al.*, manuscript in preparation), most of which accompany the amplification of the *N-myc* gene. The three *ALK*-amplified neuroblastoma cell lines showed constitutive activation of full-length ALK and the increased local concentration of receptor tyrosine kinases appeared to interfere with signals from other RTKs. It is possible that ALK-ShcC signal activation has additional effects on the malignant tumor progression of neuroblastoma, probably similar to the mechanism reported in EGFR and Neu/ErbB2 (Andrechek *et al.*, 2000; Pawson *et al.*, 2001).

To clarify the role of hyperphosphorylated ShcC in neuroblastoma cells, the 3YF-ShcC mutant, which has phenylalanines at three Grb2-binding tyrosines (Y221/222/304) of ShcC, was utilized in this study in the expectation of a dominant-negative effect specific for signals originating from the ShcC-Grb2 complex. The biological effects of the 3YF-ShcC mutant as well as wild-type ShcC and the ΔSH2 ShcC mutant, which lacks the SH2 domain, were analysed to elucidate both Grb2-dependent and -independent functions of ShcC in neuroblastoma.

Results

Suppression of ERK1/2 and Akt activation in NB-39-nu cells by expression of 3YF-ShcC

A neuroblastoma cell line, NB-39-nu, was used in this study because it shows high tumorigenicity and anchorage independency with prominent phosphorylation level of ShcC caused by constitutively activated ALK kinase. The expression level of ShcC is relatively low among the neuroblastoma cell lines examined in our previous study. T7-tagged ShcC constructs containing the full length of human ShcC cDNA (ShcC-wt), a tyrosine-to-phenylalanin mutant for all three putative Grb2-binding sites (3YF-ShcC), and the SH2-deletion mutant (ΔSH2-ShcC) were subcloned into a mammalian expression vector, pcDNA3.1. Multiple independent clones of NB-39-nu cell lines stably expressing these ShcC mutants at comparable levels were selected and submitted to biochemical and biological analysis. Results of representative clones are shown in Figure 1a, although basically same results were obtained from other independent clones (data not shown). Tyrosine phosphorylation of the 3YF-ShcC was significantly suppressed suggesting that the three tyrosines lost in this mutant are the main phosphorylation sites of ShcC in NB-39-nu (Figure 1a). As expected, the complex formation of 3YF-ShcC with Grb2 was impaired, regardless of EGF stimulation, compared with that of ShcC-wt and ΔSH2-ShcC (Figure 1c). The activation level of ERK1/2 at 5 min after the EGF stimulation was decreased by expression of 3YF-ShcC, while expression of ShcC-wt or ΔSH2-ShcC did not affect the levels of ERK1/2 activation compared with the control cells transfected only by expression vector (mock) (Figure 1d). The phosphorylation level of Akt at Ser-473 was also suppressed by expression of 3YF-ShcC, although not at a similar level as that of cells treated with Wortmannin (Sigma), a PI3K inhibitor (Figure 1e). These analyses were performed using at least two independent clones. It was confirmed that 3YF-ShcC-expression has a dominant-negative effect on the PI3K/Akt pathway as well as the Ras/ERK pathway in this neuroblastoma cell line.

Expression of 3YF-ShcC increased susceptibility to retinoic acid (RA)-induced apoptosis in NB-39-nu cells

There were no obvious differences in growth rate among the NB-39-nu clones expressing each ShcC mutant (Figure 2a), whereas the rate of [^{3}H]-thymidine incorporation of the cell lines expressing 3YF-ShcC was slightly lower than that of other cells (Figure 2b).

The cytological analyses of the cells cultured with 10 μM of all-*trans*-RA revealed that 3YF-ShcC expressing cells were more susceptible to RA-induced apoptosis than the control or ShcC-wt-expressing cells (Figure 3a). Treatment of NB-39-nu cells, especially ShcC-wt-expressing cells, with RA at a lower concentration of 2.5 or 5 μM induced mild neurite formation, flattened, substrate-adherent cells resembling epithelial cells within 48 h (Figure 3b), which is known to be a characteristics of RA-induced morphologic differentiation (Sidell *et al.*, 1983). In contrast, this type of differentiation was not observed in 3YF-ShcC-expressing cells. Along with the suppressive effects of 3YF-ShcC to the Akt pathway (Figure 1e), these results suggest that phosphorylated ShcC plays significant role in survival signals through the putative Grb2-binding sites in NB-39-nu cells.

ShcC plays a distinct role in the migration of ALK-ShcC-activated neuroblastoma cells

Expression of 3YF-ShcC significantly suppresses cell migration ability as shown by the wound-healing assay (Figure 4a). A modified Boyden chamber cell-migration assay without Matrigel using fibronectin as a chemoattractant showed the results consistent with those obtained in the wound-healing assay (Figure 4b). A similar assay with Matrigel coating on a chamber filter to evaluate the chemotactic invasive activity of each transfectant also showed decreased invasive activity in 3YF-ShcC-expressing cells (Figure 4c). In contrast, ShcC-wt expression increased the migration ability of NB-39-nu cells both in wound healing assay and modified Boyden chamber assay without Matrigel (Figure 4a, b), while the ΔSH2-ShcC expression presented no remarkable effects on the cell motility. The invasive activity of ShcC-wt-expressing cells was not significantly high compared to that of the control or of the ΔSH2-ShcC-expressing cells (Figure 4c).

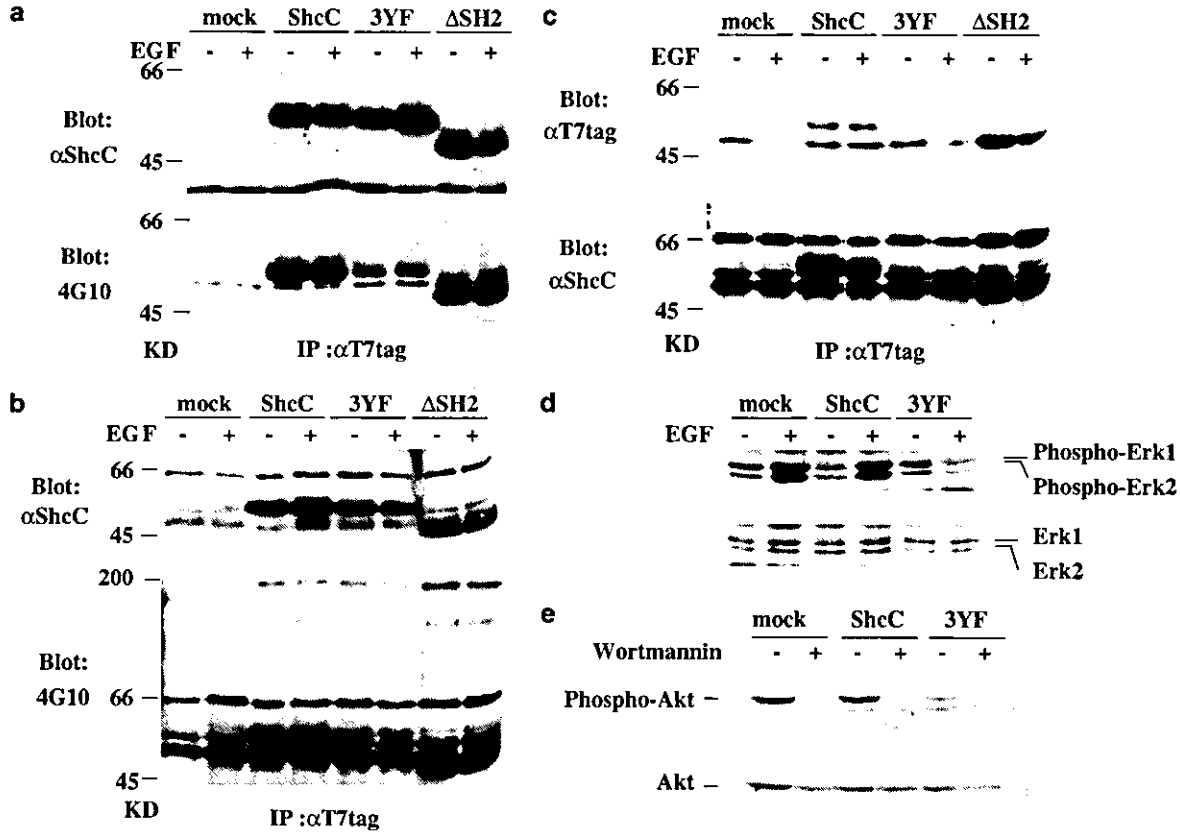

Figure 1 NB-39-nu cells stably expressing ShcC mutants analysed by immunoblotting. (**a**) Expression (upper panel) and tyrosine phosphorylation (lower panel) of ectopic ShcC mutant proteins (mock: control, ShcC: ShcC-wt, 3YF: 3YF-ShcC and ΔSH2: ΔSH2-ShcC) in the NB-39-nu cells. (**b**) Expression (upper panel) and tyrosine phosphorylation (lower panel) of both endogenous ShcC and ectopic ShcC mutants in NB-39-nu cells. (**c**) The complex formation of Grb2 with ShcC (lower panel) or ectopic ShcC mutants (upper panel) was analysed. (**d**) The activation of ERK1/2 in ShcC mutant cells. (**e**) Akt (Ser473) phosphorylation in ShcC mutant cells in a tissue culture medium with 10% fetal calf serum (FCS). For the negative control, the cells were treated with 1 μM of Wortmannin for 2 h. EGF stimulations were performed as described in Materials and methods. Lysates were duplicated and detected by the antibodies shown in the figure

Expression of ShcC-wt or 3YF-ShcC has a negative effect on the transforming activity of NB-39-nu cells

Cells expressing ShcC-wt or 3YF-ShcC tend to grow to confluence with a monolayer appearance, making a clear difference from original NB-39-nu cells that tend to form cell aggregations on the culture dishes (Figure 5a). In addition, control NB-39-nu cells and ΔSH2-ShcC-expressing cells form a considerable number of colonies in soft agar (Figure 5b), which is significantly suppressed by the expression of ShcC-wt or 3YF-ShcC (Figure 5b). These results indicate that ShcC-wt or 3YF-ShcC have inhibitory effect on the transforming activity of NB-39-nu cells, especially anchorage-independent growth. Since the overexpression of ShcC had no significant effect on the activation of ERK1/2 or Akt in our experiment, it was suggested that a unique signaling pathway rather than classical Grb2-Ras pathway is involved in this phenomenon.

Src family kinases (SFKs) are well known to be associated with the ability to induce cellular transformation including anchorage independency (Parsons and Weber, 1989; Windham *et al*., 2002). During the investigation of ShcC mutant cells in the suspension state, we noticed that the sustained activation of both Fyn and c-Src observed in the control cells and ΔSH2-ShcC-expressing cells was suppressed by the expression of ShcC-wt or 3YF-ShcC (Figure 6a, b) at 24 h after cell detachment. Especially, the condition of phosphorylation of Fyn at suspension culture well correlated with anchorage independency of NB-39-nu sublines (Figure 6a). Tendency of phosphorylation of Src Tyr-416, which indicates the kinase activation of SFKs, is consistent with these results (Figure 6c). Phosphorylation of Cas, a main substrate of SFKs, in a suspended condition has recently been associated with the anchorage-independent growth of cancer-like lung adenocarcinoma (Wei *et al*., 2002). Sustention and temporary elevation of the Cas phosphorylation was also observed specifically in the original NB-39-nu cells, control and ΔSH2-ShcC-expressing cells, whereas there was a marked decrease of the phosphorylation level of Cas in ShcC-wt- and 3YF-ShcC-expressing cells (Figure 6d, e). Treatment of NB-39-nu control cells with PP2, a Src-specific inhibiter, suppressed the phosphorylation of Cas both in an attached and suspended condition, suggesting